An alternative determination of the LEP beam energy & Calorimetry for the ILC

Chris Ainsley

<ainsley@hep.phy.cam.ac.uk>

UNIVERSITY OF CAMBRIDGE

CALICE

Calorimeter for ILC

Part 1: An alternative determination of the LEP beam energy

- Why verify the beam energy?
- The standard approach.
- The alternative approach:
  - method;
  - systematic errors;
  - results;
  - conclusions.

Why determine the beam energy accurately?

- Accurate knowledge of beam energy (E_b) important for many precision measurements at LEP.
- Relevant for measurement of $\int \mathcal{L}\, dt$ via Bhabha cross-section $\propto 1/E_b^2 \Rightarrow$ fundamental to all cross-section determinations:

$$\frac{\Delta\sigma}{\sigma} = \frac{2\Delta E_b}{E_b} .$$

- Vital for accuracy of m_W measurement—a main objective of LEP II program $\rightarrow$ resolution improved through kinematic fit constraints:

$$\frac{\Delta m_W}{m_W} = \frac{\Delta E_b}{E_b} .$$

The standard LEP energy calibration

- Measured at LEP I energies (E_b ~ 45 GeV) by resonant depolarization (RDP).
- Relies on ability to generate LEP beams with detectable spin polarizations.
- Polarization can be destroyed by oscillating B-field when in phase with spin precession.
- At resonance, can infer the "spin-tune", ν:

$$\nu = \frac{f_{prec}}{f_{rev}} = \frac{g_e - 2}{2} \cdot \frac{E_b}{m_e c^2}$$

- RDP works up to E_b ~ 60 GeV, but fails at LEP II energies (E_b ~ 100 GeV).
- At LEP II, fit lower energy RDP measurements with $E_b = a + bB$; deduce E_b from B-field (using NMR probes) at physics energies $\rightarrow$ magnetic extrapolation.
- Yearly uncertainty on E_b ~ 20 MeV; is this reliable?

The radiative return approach

- Select fermion-pair events which exhibit "radiative return to the Z" (resonant enhancement)…

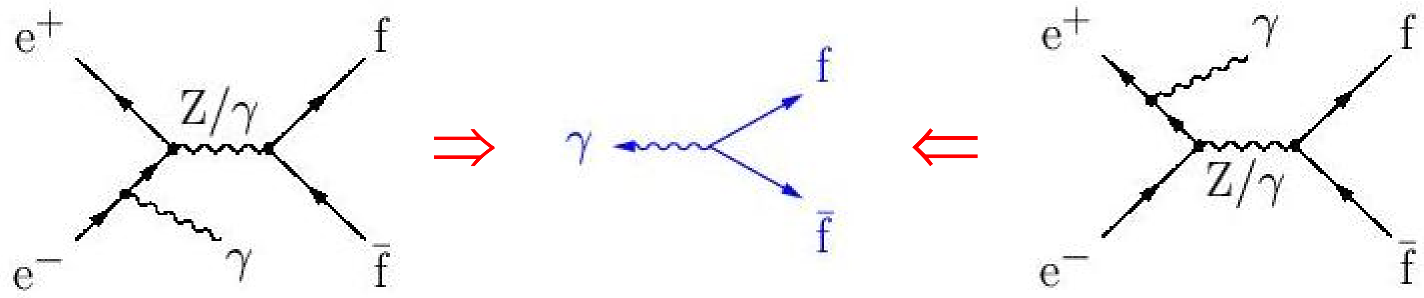

…and construct:

$\sqrt{s'}$ = $f\bar{f}$ invariant mass (f = q, e^-, μ^-, τ^-)

= Z/γ propagator mass

= centre-of-mass energy after initial-state radiation (ISR).

- $\sqrt{s'}$ sensitive to E_b through energy and momentum constraints in kinematic fits.
- Use events with $\sqrt{s'} \sim m_Z$ to reconstruct 'pseudo'-Z peak in MC (E_b known exactly) and in data (E_b inferred by measurement).
- Attribute any relative shift between peaks to a discrepancy in the measurement of the beam energy: ΔE_b.

$\sqrt{s'}$ reconstruction

- Hadronic channel:
  - Invoke standard hadronic selection.
  - Identify all isolated photons.
  - Force remaining system into jets (Durham scheme).
  - Apply kinematic fit without/ with unseen photon(s) along $\pm z$, using jet energies and angles, and $(E, \vec{p})$ conservation.
  - Retain events with exactly one reconstructed photon (either in Ecal or along $\pm z$).
  - Compute $\sqrt{s'}$ from jet energies and momenta:
    $\sqrt{s'} = m_{\text{jet-jet}}$.

- Leptonic channels:
  - Invoke standard leptonic selection.
  - Identify highest energy isolated photon; if no photons found, assume one along $\pm z$.
  - Treat event as having 3 final-state particles: $\ell^+\ell^-\gamma$.
  - Compute $\sqrt{s'}$ from angles alone, imposing $(E, \vec{p})$ conservation:
    $$\frac{s'}{s} = \frac{\sin\chi_1 + \sin\chi_2 - |\sin(\chi_1+\chi_2)|}{\sin\chi_1 + \sin\chi_2 + |\sin(\chi_1+\chi_2)|}.$$

Reconstructed $\sqrt{s'}$ distributions

- 1997–2000 OPAL data:

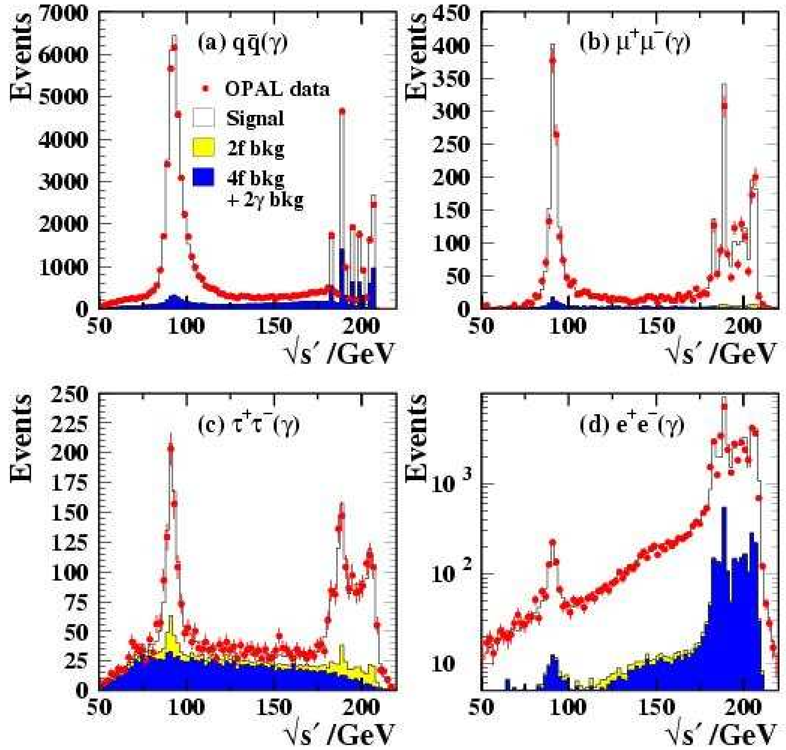

- Dominated by radiative-return and full-energy events.
- (a) $q\bar{q}\gamma$: high statistics, b/g ~ 4 % under peak → mainly $q\bar{q}e^+e^-$ (resonant); $\sqrt{s'}$ resolution ~ 2 GeV.
- (b) $\mu^+\mu^-\gamma$: lower statistics, but very low b/g and excellent angular resolution.
- (c) $\tau^+\tau^-\gamma$: low efficiency, worse resolution and larger b/g.
- (d) $e^+e^-\gamma$: small signal, dwarfed by *t*-channel contribution.

Fitting the peak

- Analytic function fitted to reconstructed √s′ distribution in MC at known $E_b = E_b^{MC}$ around 'pseudo'-Z peak.
- Same function fitted to reconstructed √s′ distribution in data, assuming $E_b = E_b^{LEP}$ (normalization/peak position free to vary).

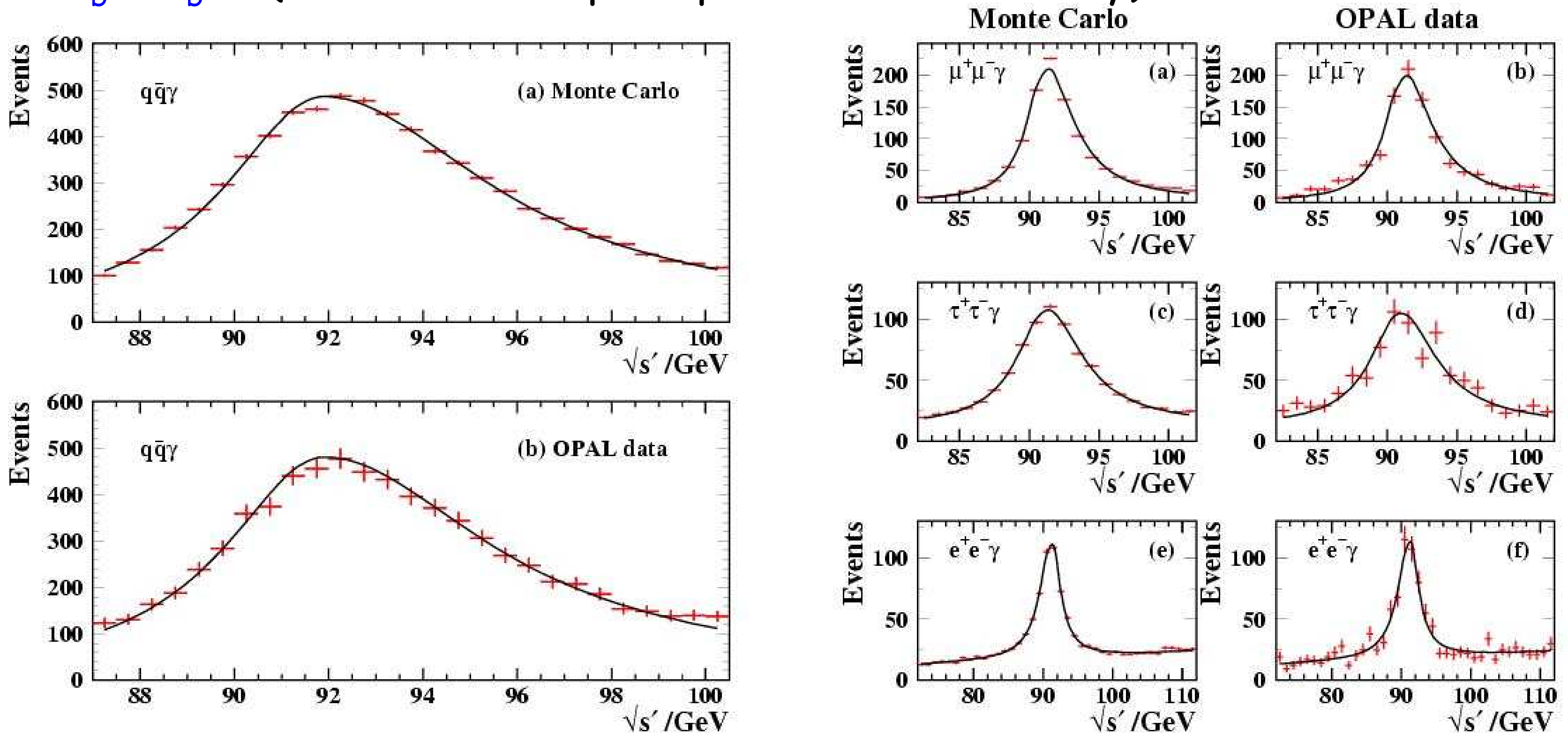

Extraction of beam energy (e.g. $q\bar{q}\gamma$ channel)

- Repeat function fitting in data as a function of assumed discrepancy, $\Delta E_b = E_b^{OPAL} - E_b^{LEP}$ (= −450, −300, −150, 0,+150,+300 MeV); use peak position (M^*) to characterize overall $\sqrt{s'}$ energy scale. E.g. 1998 data:

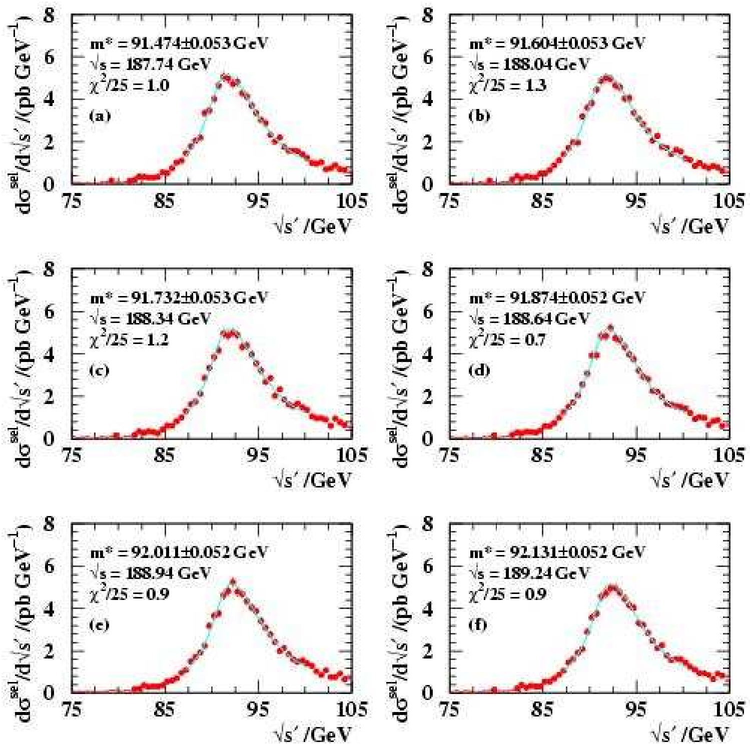

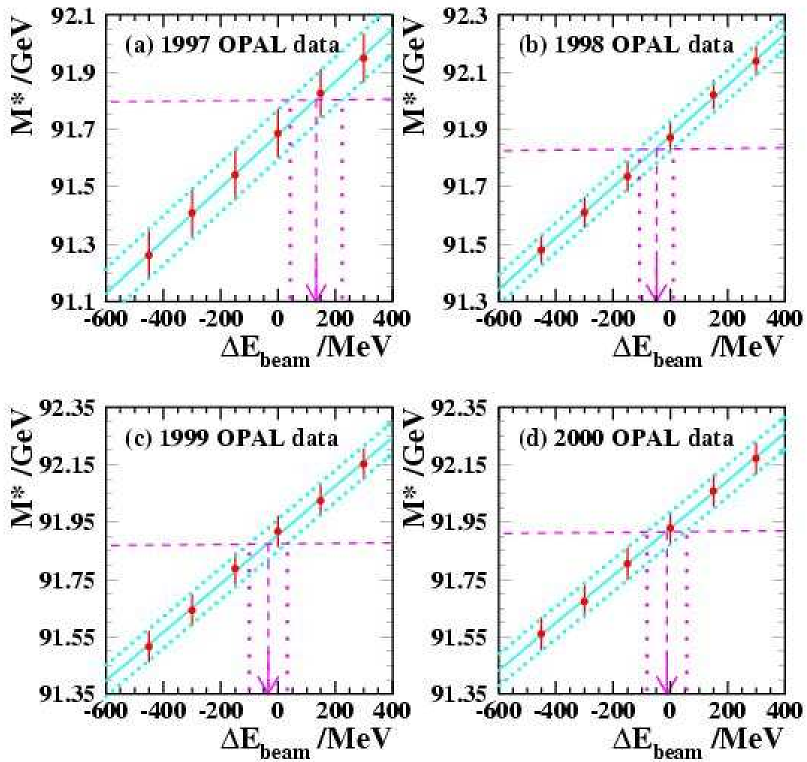

- Extract optimum value of ΔE_b where M^* in data matches MC expectation.

Chris Ainsley
<ainsley@hep.phy.cam.ac.uk>

Dominant systematic errors

- Hadronic channel:

Effect	Error /MeV
Detector modelling	34
(jet mass scale	25)
(jet energy scale	17)
(photon energy scale	12)
(jet angular scale	9)
(other	7)
Fragmentation/hadronization	16
Fit parameters	3
ISR modelling	3
Backgrounds	1
I/FSR interference	1
Beam energy spread/boost	1
Total	**38**
Monte Carlo statistics	5
LEP calibration	11
Full Total	**40**

- Leptonic channels:

Effect	Error /MeV		
	$\mu^+\mu^-\gamma$	$\tau^+\tau^-\gamma$	$e^+e^-\gamma$
Lepton angular scale	21	66	24
Lepton angular resolution	2	4	7
Fit parameters	1	4	10
ISR modelling	1	7	10
Non-resonant background	< 1	6	4
Bhabha/t-channel	< 1	3	5
Beam energy spread/boost	2	5	6
Total	**21**	**67**	**30**
Monte Carlo statistics	9	34	34
LEP calibration	11	11	11
Full Total	**25**	**76**	**46**

Beam energy measurements

- 1997–2000 OPAL data:

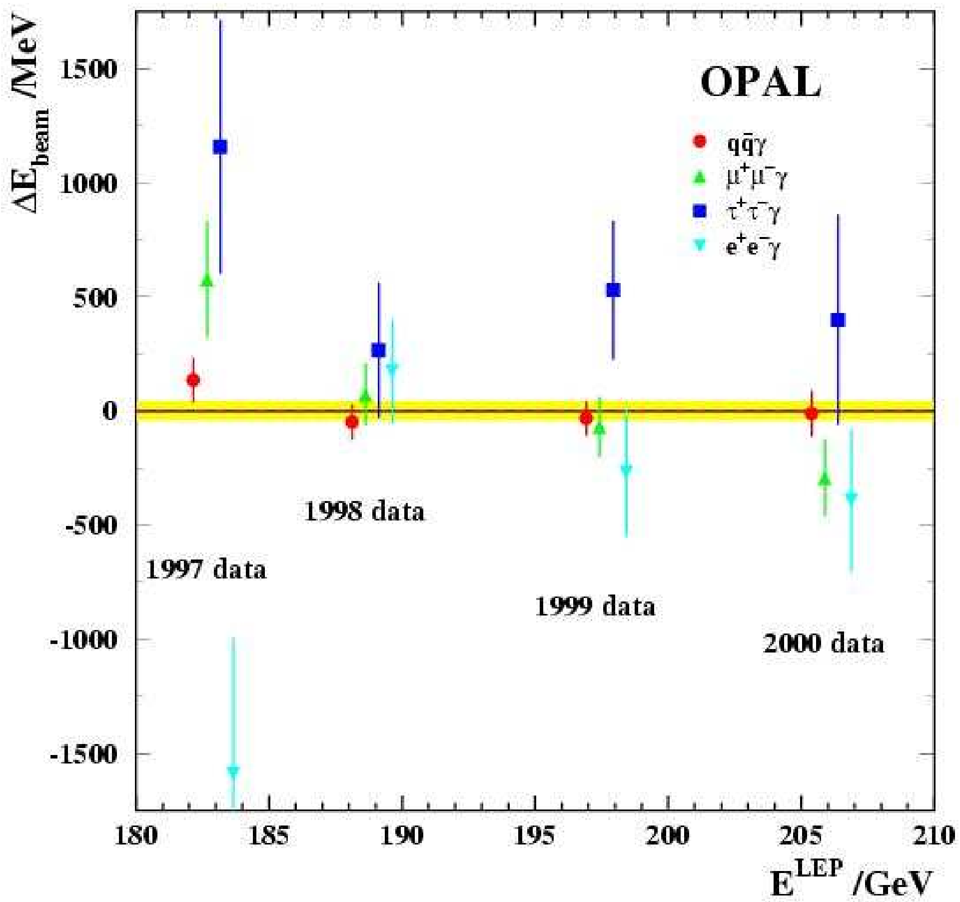

- All $q\bar{q}\gamma$ data:
  $\Delta E_b = +1 \pm 38 \pm 40$ MeV.
- All $\ell^+\ell^-\gamma$ data:
  $\Delta E_b = -2 \pm 62 \pm 24$ MeV.
  - all $\mu^+\mu^-\gamma$ data:
    $\Delta E_b = -32 \pm 75 \pm 25$ MeV.
  - all $\tau^+\tau^-\gamma$ data:
    $\Delta E_b = +313 \pm 175 \pm 76$ MeV.
  - all $e^+e^-\gamma$ data:
    $\Delta E_b = -88 \pm 146 \pm 46$ MeV.
- All $f\bar{f}\gamma$ data combined:
  $\Delta E_b = 0 \pm 34 \pm 27$ MeV.

Conclusions

- Beam energy from radiative fermion-pairs consistent with standard LEP calibration

  $\Rightarrow$ vindication for magnetic extrapolation procedure;

  $\Rightarrow$ good news for m_W determination.
- Systematic uncertainties 38 ($q\bar{q}\gamma$), 21 ($\mu^+\mu^-\gamma$), 67 ($\tau^+\tau^-\gamma$), 30 ($e^+e^-\gamma$) MeV; cf. ~ 20 MeV error on magnetic extrapolation.
- For more info, see **Phys. Lett. B 604, 31 (2004)**.
- Standard LEP approach requires circulating beams; not appropriate for a linear collider.
- Radiative return approach independent of accelerator specs $\rightarrow$ potential method for measuring E_b at a high-statistics future linear collider: the ILC.
- Possibility under investigation…

Part 2: Calorimetry for the ILC

- Why do we need the ILC?
- The physics objectives.
- The calorimeter requirements & how to achieve them.
- The CALICE program:
  - overview;
  - prototypes & test beams;
  - simulation;
  - reconstruction.

CALICE
Calorimeter for ILC

The International Linear Collider (ILC)

- Widespread worldwide support for an e^+e^- linear collider operating at $\sqrt{s}$ = 0.5–1 TeV.
- August '04: International Technology Review Panel recommended adoption of superconducting (TESLA-like) technology for the accelerator.
- Asia, Europe and North America lined up behind decision; agreed to collaborate on technical design.
- Timescale for physics set by ILC Steering Group
  - first collisions ~ 2015;
  - detector TDRs in 2009;
  - formation of experimental collaborations in 2008.
- Much to be done in next 3 years!

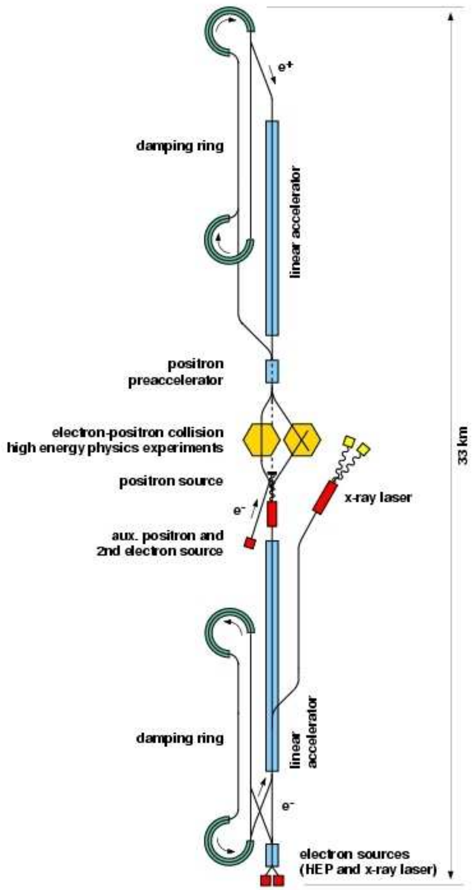

ILC/LHC synergy

- ILC will provide precision measurements (masses, branching fractions, *etc.*) of physics revealed by LHC:
  - properties of Higgs boson(s);
  - characterization of SUSY spectrum;
  - precision measurements of the top quark;
  - strong electroweak symmetry breaking;
  - much, much more…
- Overlapping running of LHC/ILC beneficial to physics capabilities of both machines ($\Rightarrow$ aim for collisions in 2015).
- Dedicated study group investigating synergy between ILC and LHC [see **LHC-LC Study Group**, **hep-ph/0410364** ~ 500 pages!]

ILC physics objectives

- Many of the "interesting" processes involve multi-jet (6/8 jets) final states, as well as leptons and missing energy.
- Accurate reconstruction of jets key to disentangling these processes.
- Small signals, e.g. $\sigma(e^+e^- \rightarrow ZHH) \sim 0.3$ pb at 500 GeV.

  $\Rightarrow$ require high luminosity.

  $\Rightarrow$ need detector optimized for precision measurements in a difficult environment.

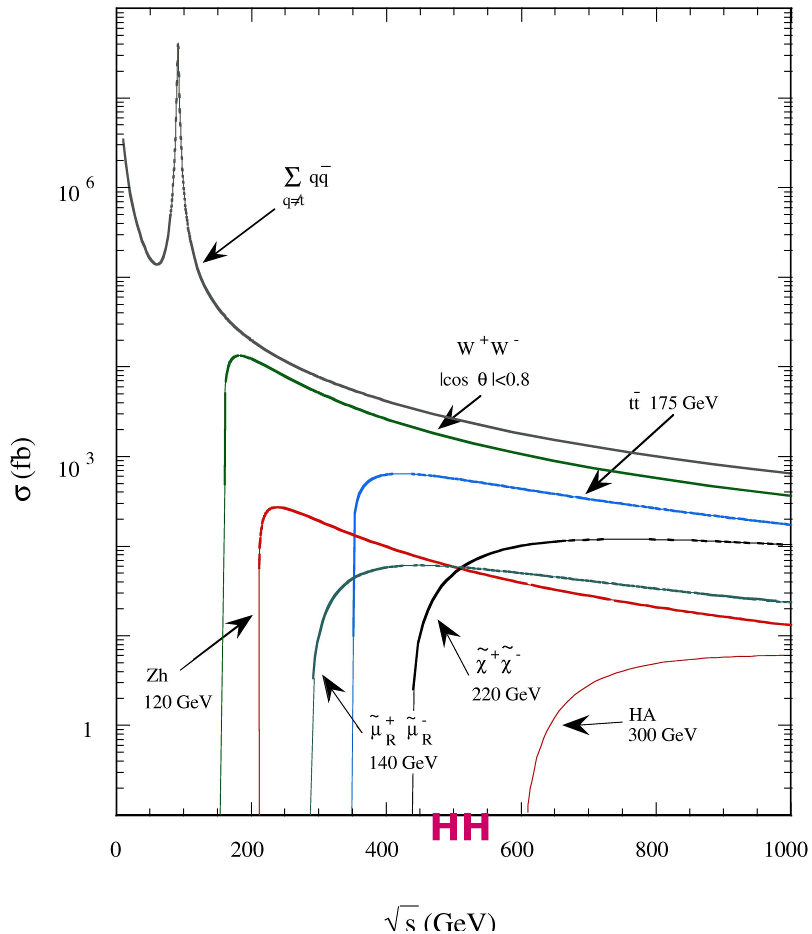

Chris Ainsley
<ainsley@hep.phy.cam.ac.uk>

Comparison with LEP

- Physics at LEP dominated by $e^+e^- \to Z$ and $e^+e^- \to W^+W^-$; backgrounds not too problematic.
- Kinematic fits used for mass (*e.g.* m_W) reconstruction $\Rightarrow$ shortcomings of jet energy resolution surmountable.
- Physics at ILC dominated by backgrounds.
- Beamstrahlung, multi-ν final states, SUSY(?)

  $\Rightarrow$ missing energy (unknown);

  $\Rightarrow$ kinematic fitting less applicable.
- Physics performance of ILC depends critically on detector performance (unlike at LEP).
- Stringent requirements on ILC detector, especially the calorimetry.
- Excellent jet energy resolution a must!

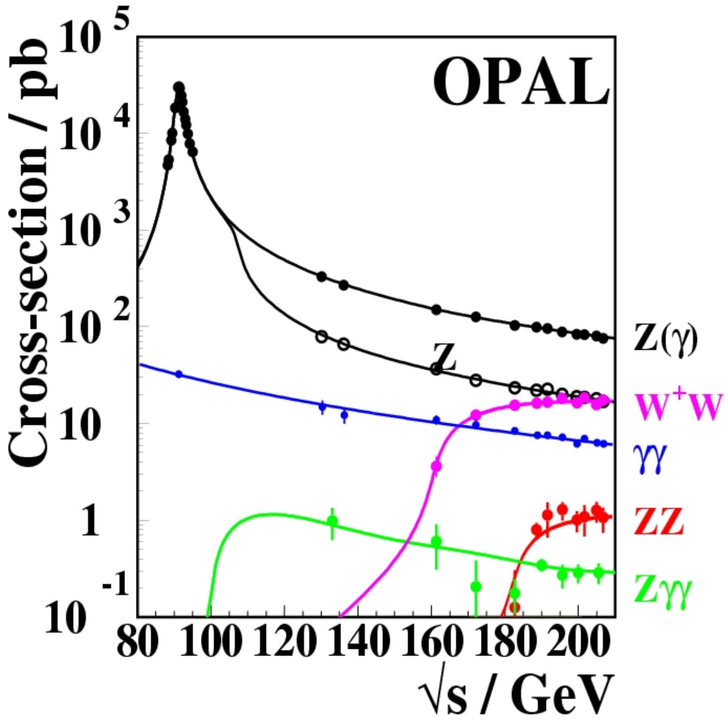

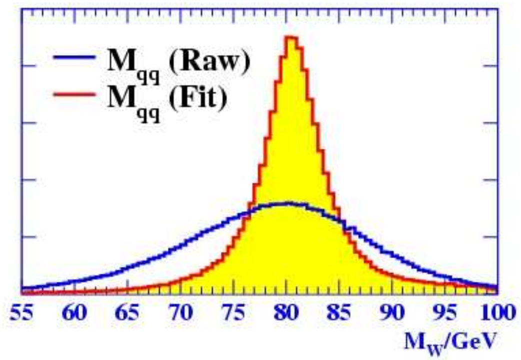

$W^{\pm}/Z$ separation at the ILC

- Jet energy resolution impacts directly on physics sensitivity.
- If Higgs mechanism not realized in nature, then QGC processes become important:

  $e^+e^- \to \nu_e\bar{\nu}_e W^+W^- \to \nu_e\bar{\nu}_e q_1q_2q_3q_4$;

  $e^+e^- \to \nu_e\bar{\nu}_e ZZ \to \nu_e\bar{\nu}_e q_1q_2q_3q_4$.
- To differentiate, need to distinguish $W^{\pm} \to qq$, from $Z \to qq$.
- Requires unprecented jet energy resolution:

  $\sigma_E/E \sim 30\%/\surd(E/\mathrm{GeV})$.
- Best acheived at LEP (ALEPH):

  $\sigma_E/E \sim 60\%/\surd(E/\mathrm{GeV})$.

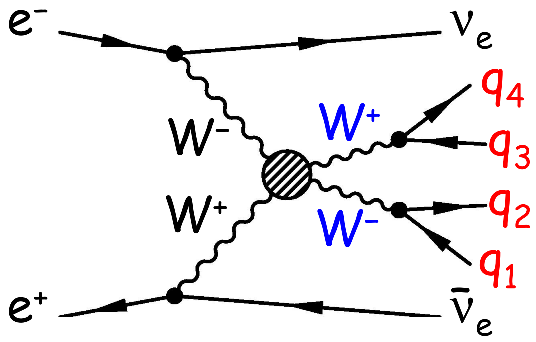

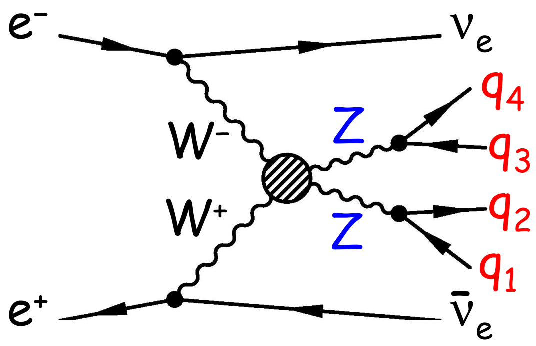

$W^{\pm}/Z$ separation at the ILC

- Plot jet$_1$-jet$_2$ invariant mass vs jet$_3$-jet$_4$ invariant mass:

LEP detector

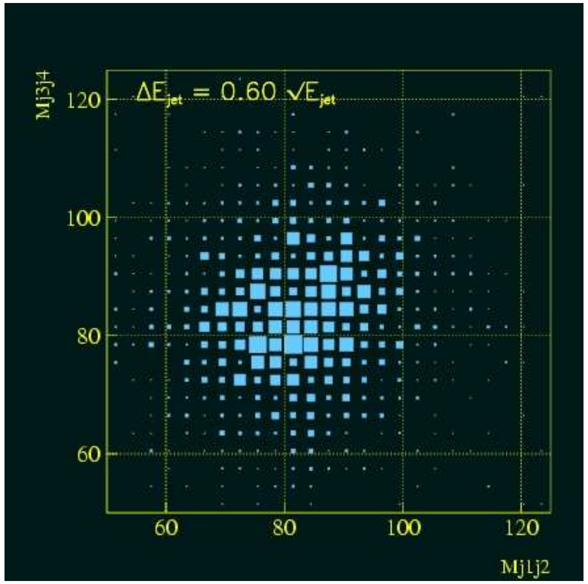

$\sigma_E/E \sim 60\%/\sqrt{(E/GeV)}$

ILC detector

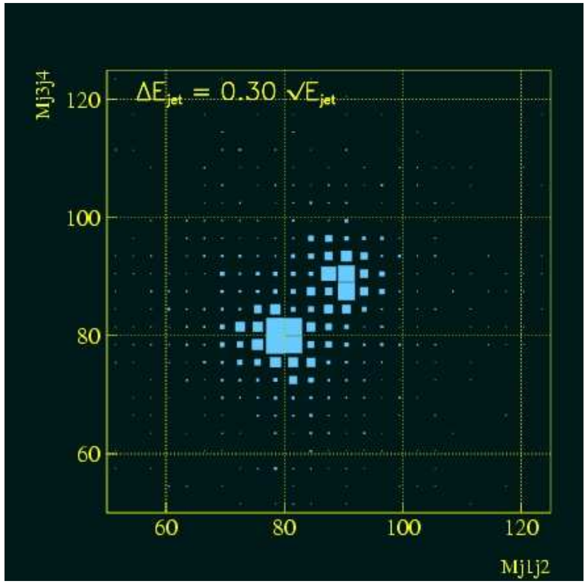

$\sigma_E/E \sim 30\%/\sqrt{(E/GeV)}$

- Discrimination between W^+W^- and ZZ final states achievable at ILC.

Higgs potential at the ILC

- If Higgs does exist, probe potential via trilinear HHH coupling in:
  $e^+e^- \to ZHH \to qqbbbb$.
- Signal cross-section small; combinatoric background large (6 jets).
- Use discriminator:

  $\mathrm{Dist} = ((M_H - M_{12})^2 + (M_z - M_{34})^2 + (M_H - M_{56})^2)^{1/2}$.

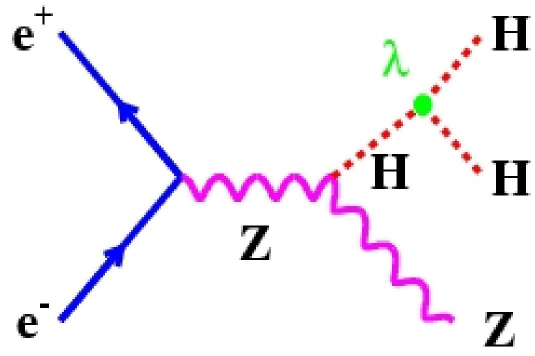

LEP detector

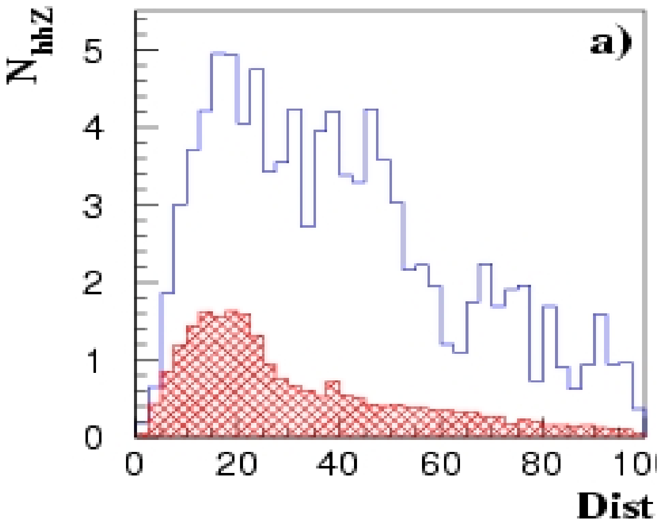

$\sigma_E/E \sim 60\%/\sqrt{(E/GeV)}$

ILC detector

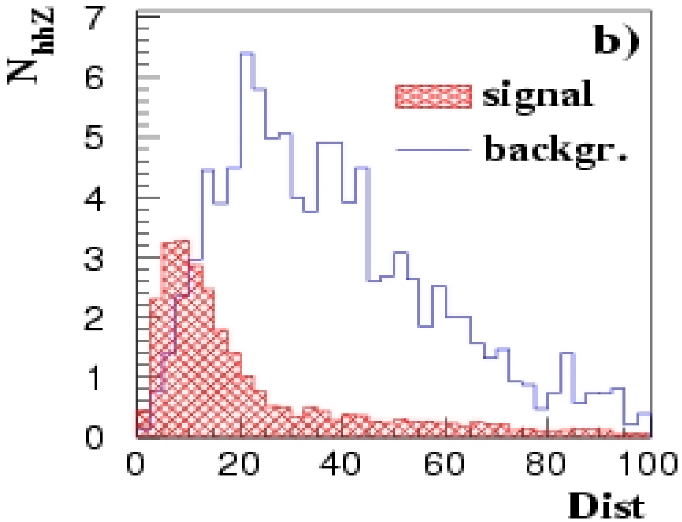

$\sigma_E/E \sim 30\%/\sqrt{(E/GeV)}$

- Measurement possible at ILC with targeted jet energy resolution.
- How can this goal actually be achieved?

The particle flow paradigm

- LEP/SLD ⇒ optimal jet energy resolution achieved through particle flow paradigm.
- Reconstruct 4-momentum of each and every particle in the event using the best-suited detector:
  - charged particles (~ 65 % of jet energy) → tracker;
  - photons (~ 25 %) → Ecal;
  - neutral hadrons (~ 10 %) → (mainly) Hcal.
- Replace poor calorimeter measurements with good tracker measurements ⇒ explicit track-cluster associations; avoiding double counting.

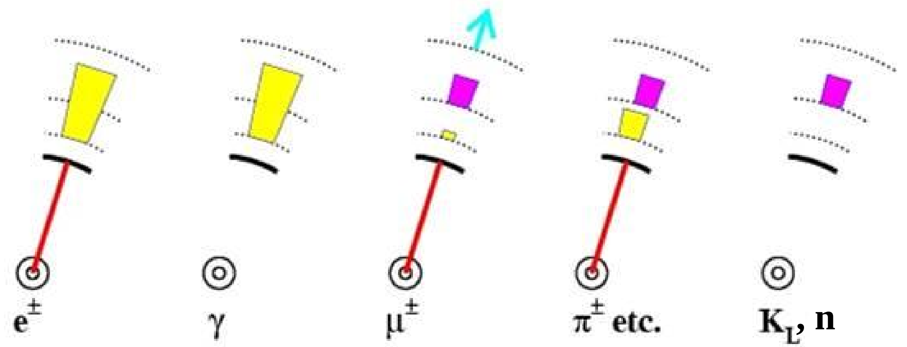

- Need to efficiently separate energy deposits from different particles in a dense environment.

The particle flow paradigm

- Jet energy resolution:
  $\sigma^2(E_{jet}) = \sigma^2(E_{ch.}) + \sigma^2(E_\gamma) + \sigma^2(E_{h0}) + \sigma^2(E_{confusion})$.
- Excellent tracker $\Rightarrow$ $\sigma^2(E_{ch.})$ negligible.
- Other terms calorimeter-dependent.
- Expect $\sigma(E_i) = A_i \surd E_i$ for i=γ,h0 ($\approx$ intrinsic energy resolution of Ecal, Hcal, respectively: $A_\gamma \sim 11$ %, $A_{h0} \sim 50$ %).
- Since $E_i = f_i E_{jet}$ ($f_\gamma \sim 25$ %, $f_{h0} \sim 10$ %):
  $\sigma(E_{jet}) = \surd\{(17\ \%)^2 E_{jet} + \sigma^2(E_{confusion})\}$.
- Ideal case, $\sigma(E_{confusion}) = 0$
  $\Rightarrow$ $\sigma(E_{jet}) = 17\ \% \surd E_{jet}$;
  $\Rightarrow$ desired resolution attainable (in principle).
- Reality dictated by wrongly assigned energy.
- Ability to separate E/M showers from charged hadron showers from neutral hadron showers is **critical**.
- Granularity (*i.e.* spatial resolution) more important than intrinsic energy resolution.

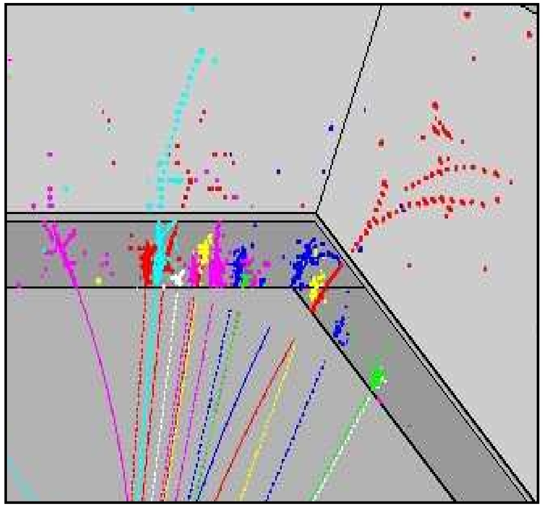

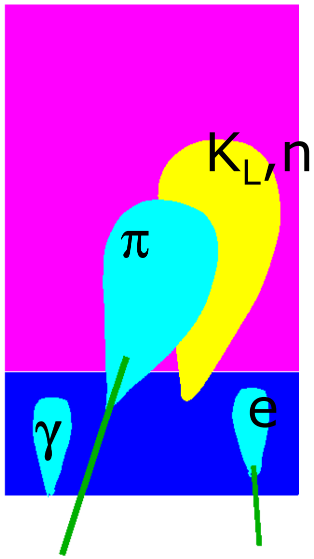

Calorimeter requirements

- Implications of particle flow on calorimeter design:
  - excellent energy resolution for jets;
  - excellent energy/angular resolution for photons;
  - ability to reconstruct non-pointing photons;
  - hermeticity.
- Need to separate energy deposits from individual particles
  $\Rightarrow$ compact, narrow showers;
  $\Rightarrow$ small X_0 and $R_{\text{Molière}}$ and high lateral granularity ~ $O(R_{\text{Molière}})$.
- Need to discriminate between E/M and hadronic showers
  $\Rightarrow$ force E/M showers early, hadronic showers late;
  $\Rightarrow$ small $X_0 : \lambda_{had}$ absorber and high degree of longitudinal segmentation.
- Need to separate hadronic showers from charged and neutral particles
- $\Rightarrow$ strong B-field (also good for retention of background within beampipe).
- Need minimal material in front of calorimeters
- $\Rightarrow$ put the Ecal and Hcal inside coil (at what cost?).

Calorimeter requirements

- Ecal and Hcal inside coil ⇒ better performance, but impacts on cost.
- Ecal → silicon-tungsten (Si/W) sandwich:
  - Si → pixelated readout, compact, stable.
  - W → $X_0 : \lambda_{had}$ ~ 1:25;
  - $R_{Molière}$ ~ 9 mm (effective $R_{Molière}$ increased by inter-W gaps) ⇒ 1×1 cm² lateral granularity for Si pads;
  - longitudinal segmentation: 40 layers ($24 X_0$, $0.9 \lambda_{had}$).
- Hcal → ??/steel (??/Fe) sandwich (?? is a major open question):
  - ?? = scintillator ⇒ analog readout (AHcal), lower granularity (~ 5×5 cm²) → electronics cost.
  - ?? = RPCs, GEMs, … ⇒ digital readout (DHcal), high granularity (1×1 cm²) → count cells hit ∝ energy (if 1 hit per cell).

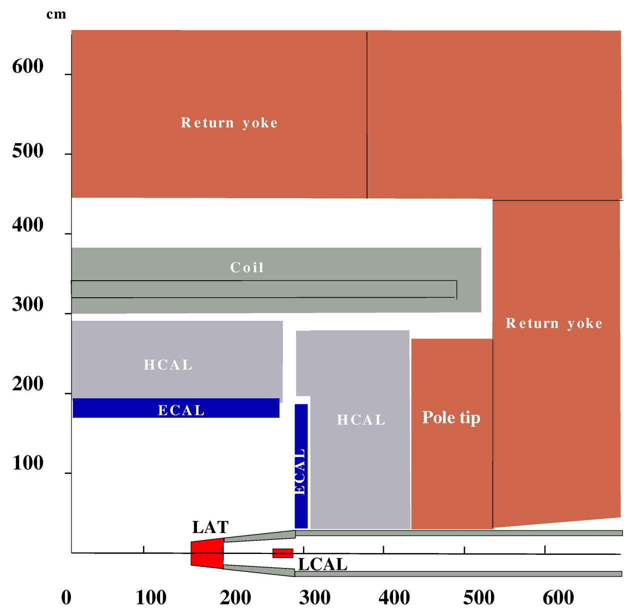

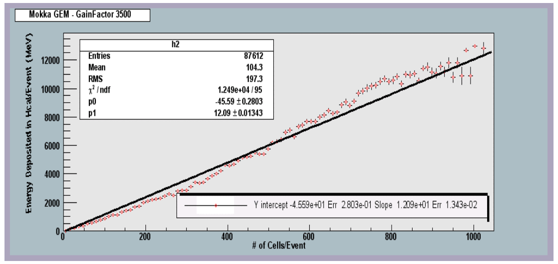

CALICE

- CAlorimeter for the LInear Collider Experiment → collaboration of 190 members, 32 institutes (Asia, Europe & North America).
- R&D on calorimetry; working towards beam tests of prototypes in a common hardware+software framework.
- Focus on high granularity, fine segmentation.
- Aims to:
  - test technical feasibility of hardware;
  - compare alternative concepts (e.g. AHcal vs DHcal);
  - validate simulation tools (especially modelling of hadronic showers);
  - prove (or disprove) the viability of a particle flow detector;
  - justify cost for high granularity.
- Pre-prototype Ecal already (mostly) built; part-tested with cosmic rays (Paris, DESY) and low energy (1–6 GeV) e^- beam (DESY).

ECAL prototype overview

- Si/W 3×10 layers; W thickness 1.4, 2.8, 4.2 mm (0.4X_0, 0.8X_0, 1.2X_0).
- Each layer → 3×3 wafers.
- Each wafer → 6×6 Si pads.

- PCB houses 12 VFE chips.
- 18 channels input to chip ⇒ 2 chips/wafer.
- 1 multiplexed output.

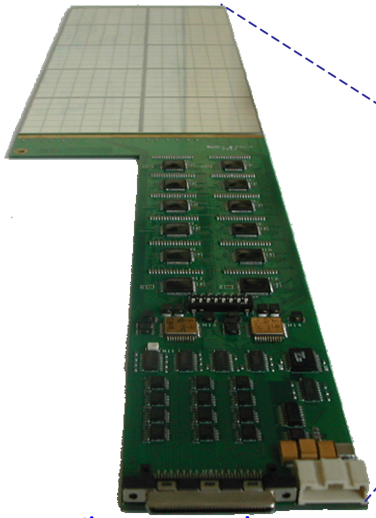

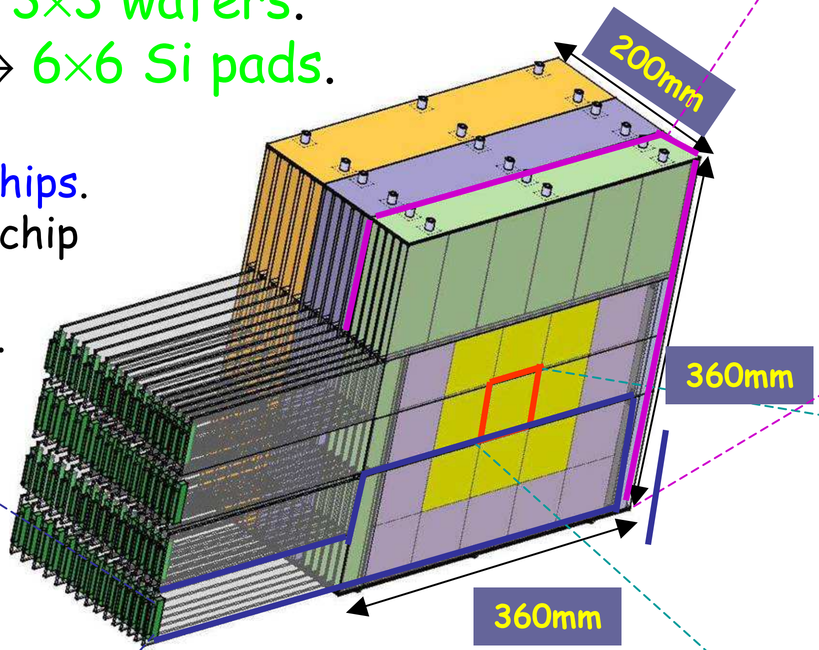

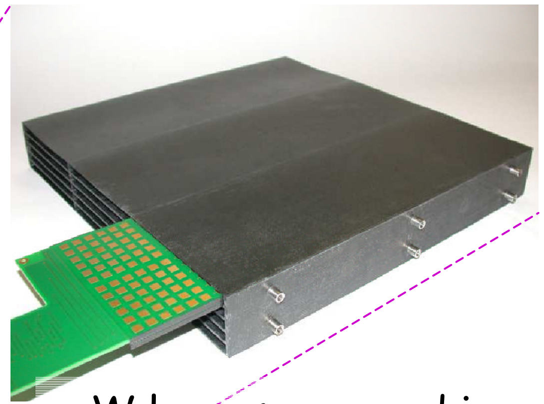

- W layers wrapped in carbon fiber.
- Si/W/Si sandwich slots into 8.5 mm alveolus.

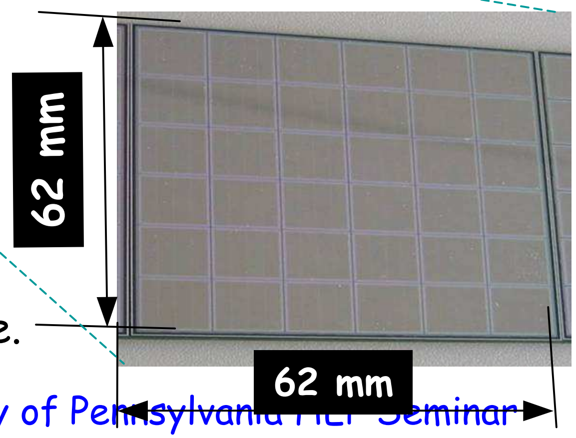

- 6x6 1x1 cm^2 (x0.5 mm) Si pads.
- Analog signal; 16-bit dynamic range.

Ecal prototype electronics

- CALICE readout card (CRC) based on CMS tracker FE driver board (saved time!).
- Designed/built by UK institutes (Imperial, RAL, UCL).
- Receives 18-fold multiplexed analog data from up to 96 VFE chips (= 1728 channels ⇒ 6 cards required for full prototype).
- Digitizes; on-board memory to buffer ~ 2000 events during spill.
- AHcal plan to use same CRCs.

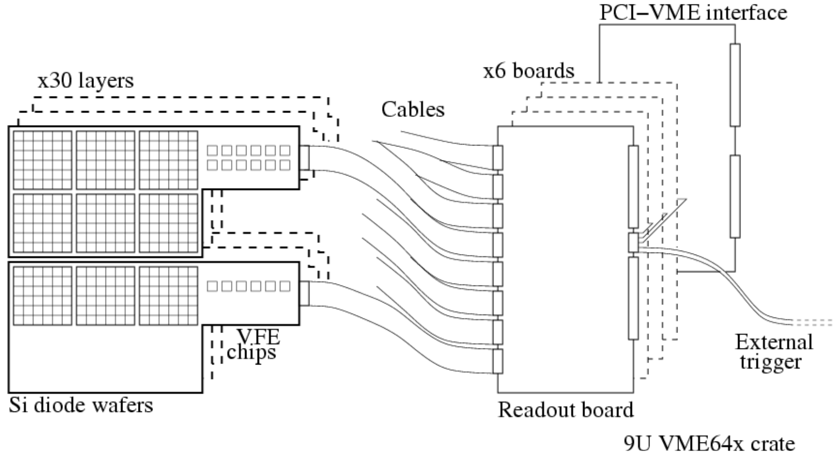

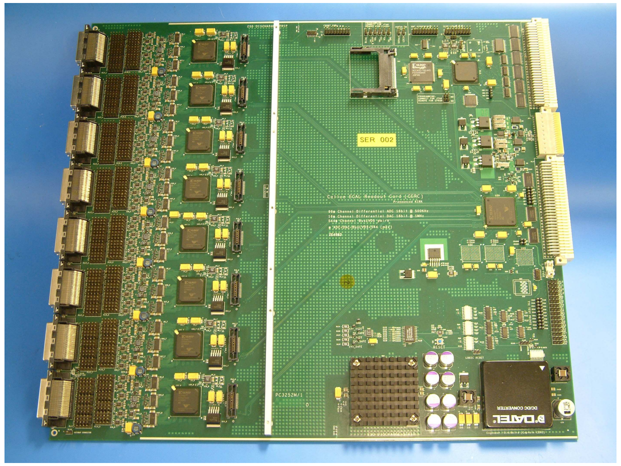

Cosmic ray tests

- Cosmic calibration, Dec. 2004 (LLR, Paris).
- E.g. of response vs ADC value for 6×6 cm² wafer (36 1×1 cm² Si pads) → Gaussian noise; Landau signal (mip):

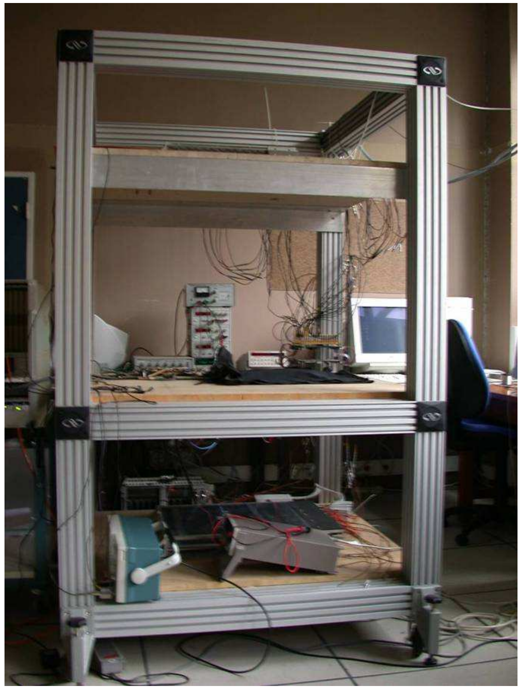

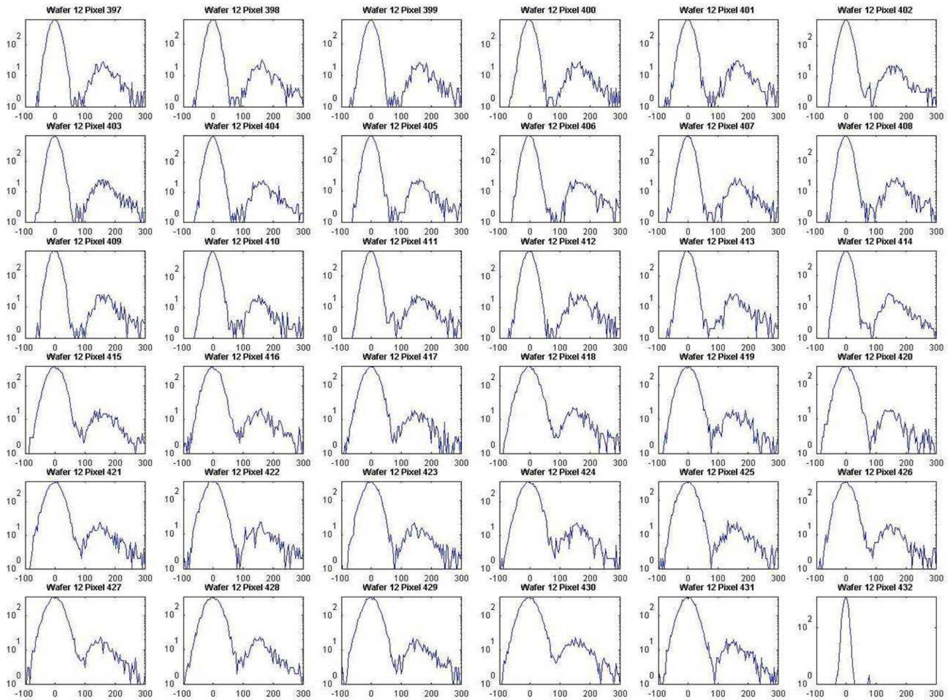

Cosmic ray tests

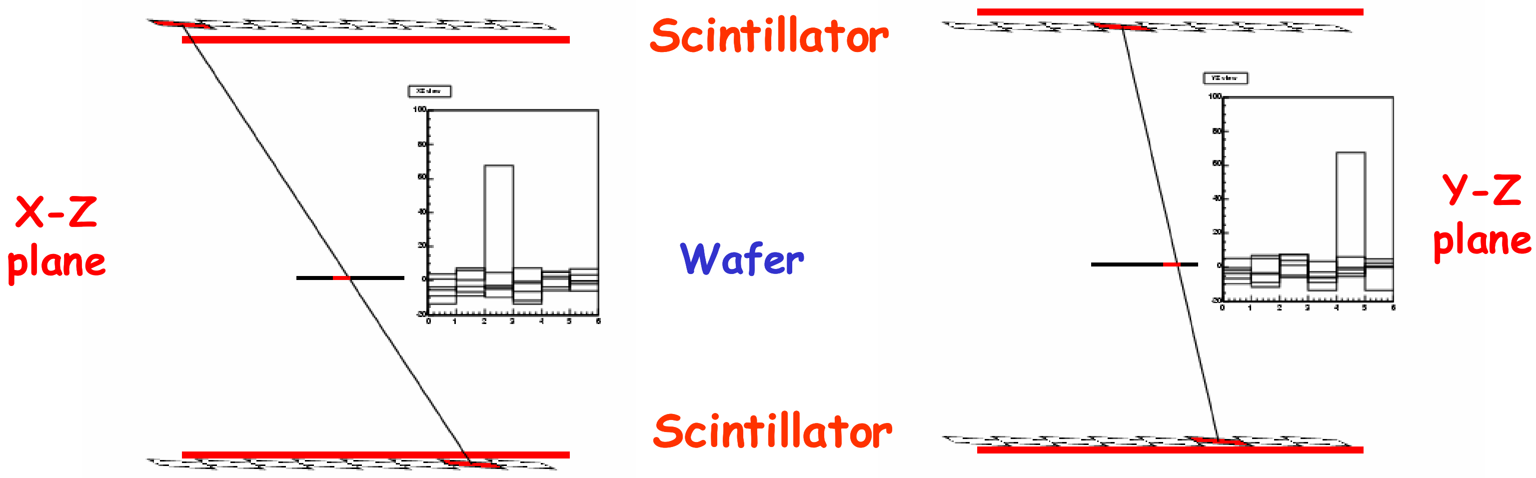

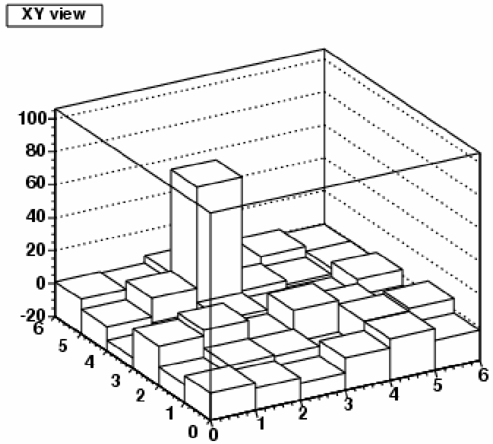

- E.g. of cosmic ray event.
- Single Si wafer; full read-out chain.
- Triggered by coincidence in scintillators.
- Track extrapolated through Si wafer.
- See clear signal over background.

Cosmic ray tests

- 10 layers assembled, Dec. 2004 (LLR, Paris).
- > 10^6 events recorded over Xmas (unmanned).
- Signal/noise ~ 9.
- This event: Jan 4, 2005.

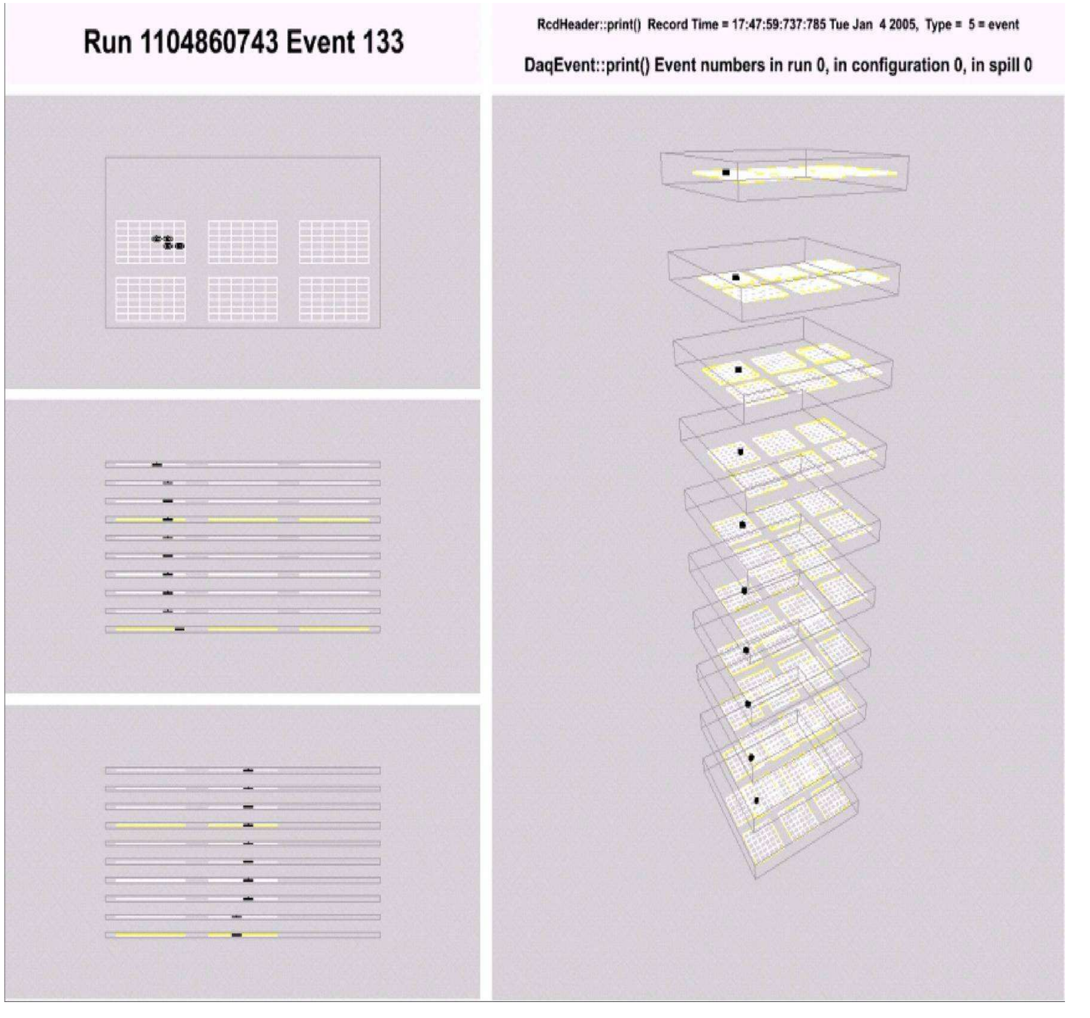

Beam tests

- Jan. 12, '05
  Ecal hardware moved to DESY.
- Jan. 13–14
  14 layers, 2×3 wafers/layer assembled ⇒ 84 wafers total ⇒ 3024 Si pixels (1/3 complete).
- Jan. 17
  First e^- beam recorded, triggered by drift chamber (200 μm resolution).
- Jan. 18
  This event (6 GeV e^-):

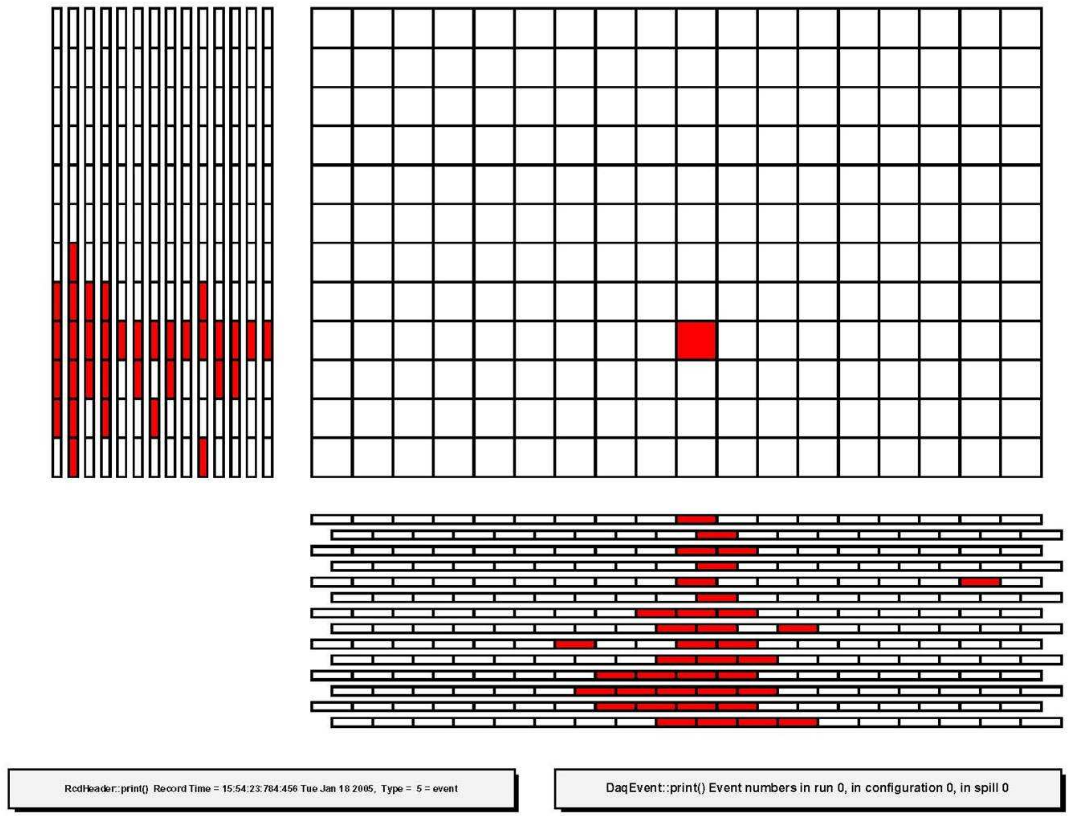

CALICE test beam schedule

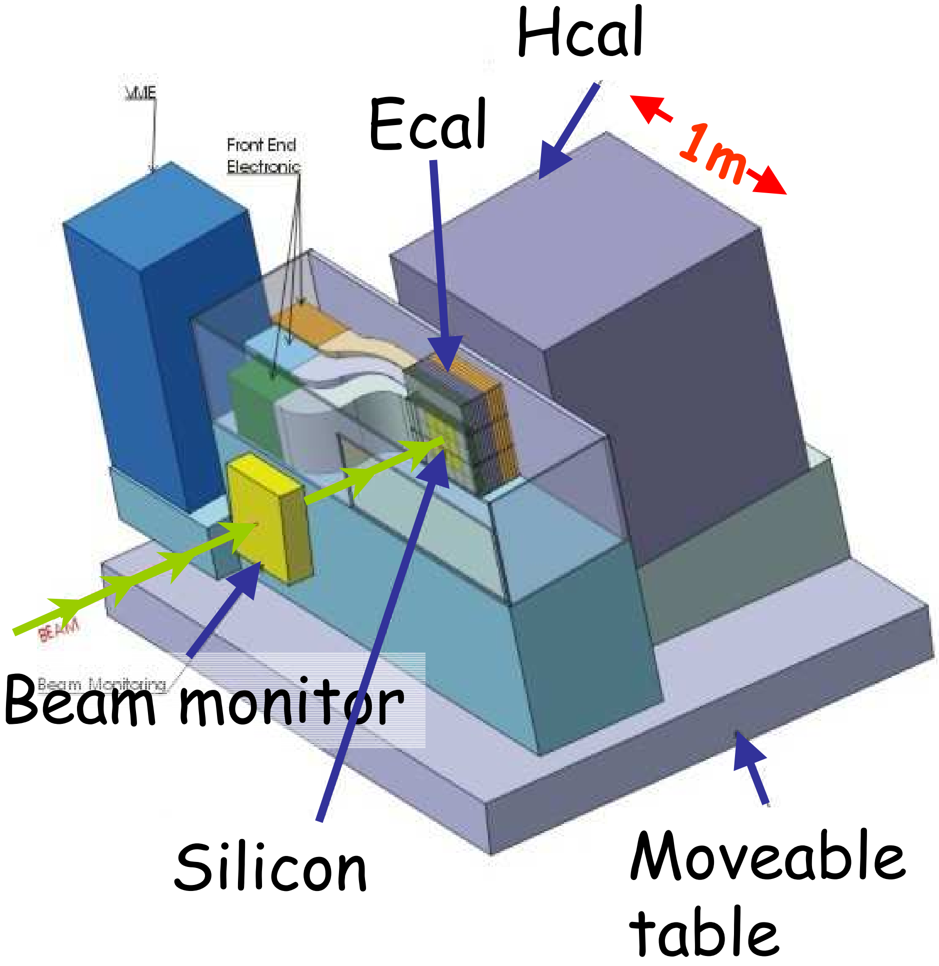

- 10-12/2005
  ECAL only, cosmics, DESY.
- 1-3/2006
  6 GeV e^- beam, DESY (complete ECAL: 9720 channels).
- 9-11/2006
  Physics run at CERN, with AHcal.
- mid-2007
  To FNAL MTBF.
- ECAL: 30 layers W+Si.
- HCAL: 40 layers Fe +
  - "analogue" tiles:
    - scintillator tiles;
    - 8k, 3x3 cm^2 –12x12 cm^2.
  - "digital" pads:
    - RPCs, GEMs;
    - 350k, 1x1 cm^2.

Simulation

- Hadronic shower development poorly understood in simulation.
- Geant3 (histo) and Geant4 (points) show basic differences.

1 GeV π^+

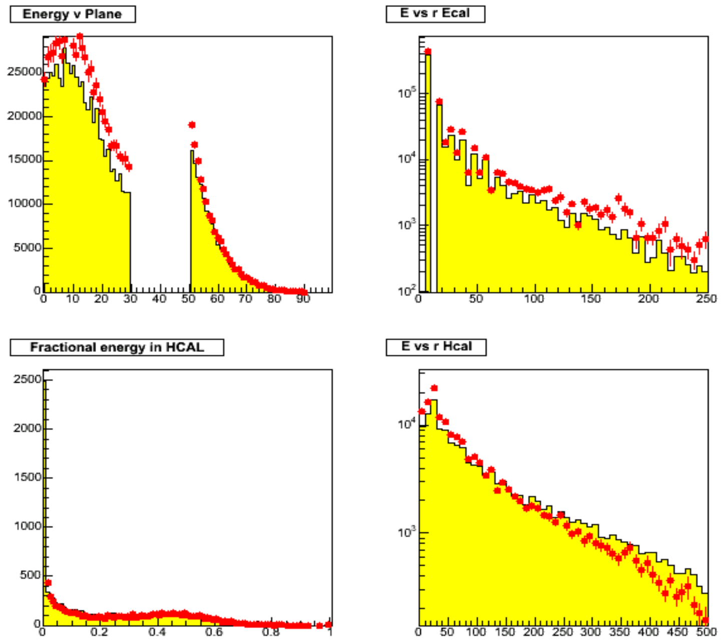

50 GeV π^+

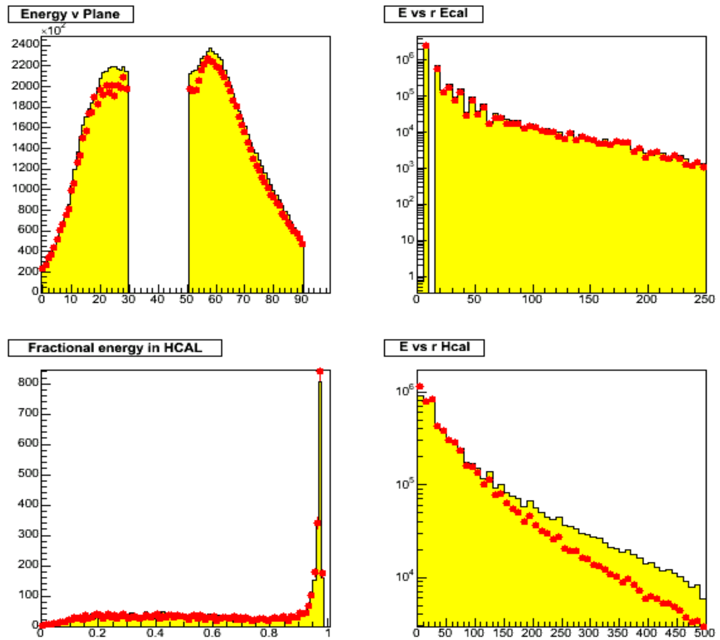

- Need reliable simulation to optimize proposed detector for ILC.
- Use test beam data to critically compare different models.

Comparing the models

- Compare G3 and G4 (and Fluka) with different hadronic shower models.
- E.g. **10 GeV** π^-; Si/W Ecal, RPC/Fe Hcal:

cells hit (normalized)   Energy deposited (normalized)

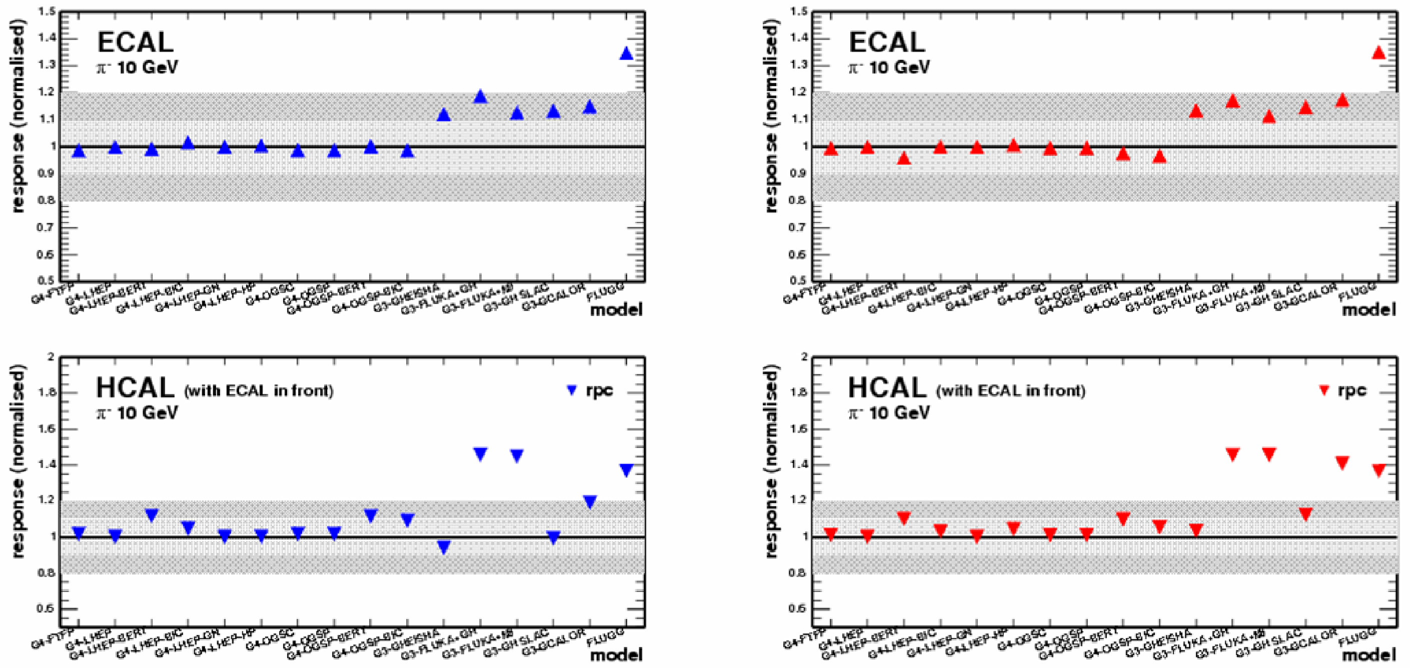

- Ecal shows some E/M discrepancies, but general consistent behavior.
- Hcal variation much more worrisome.

Comparing the models

- Extend to comparison between RPC and scintillator Hcal alternatives.

cells hit (normalized) | Shower width (normalized)

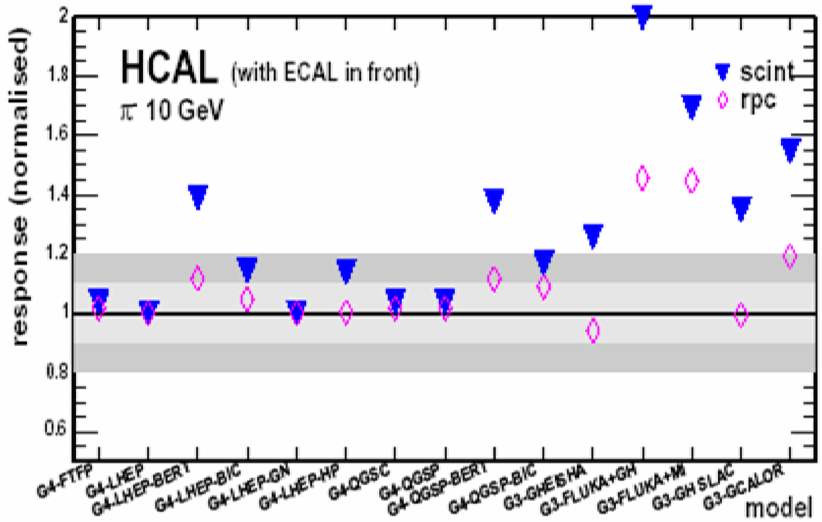

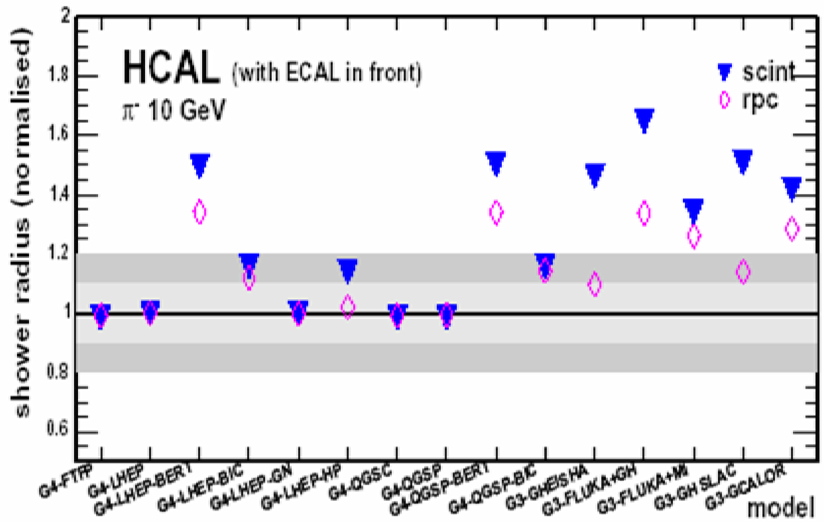

- RPC Hcal less sensitive to low energy neutrons than scintillator Hcal.
- Enforces need for test beam data.
- Guides test beam strategy (energies, statistics, *etc.*).

Calorimeter cluster reconstruction

- Reconstruction software development heavily reliant on simulation.
- Essential for detector optimization studies.
- Highly granular calorimeter → **very different** from previous detectors.
- Shower-imaging capability.
- Requires **new approaches** to cluster reconstruction.
- Must have minimal ties to geometry.
- Ingenuity will dictate success of particle flow.

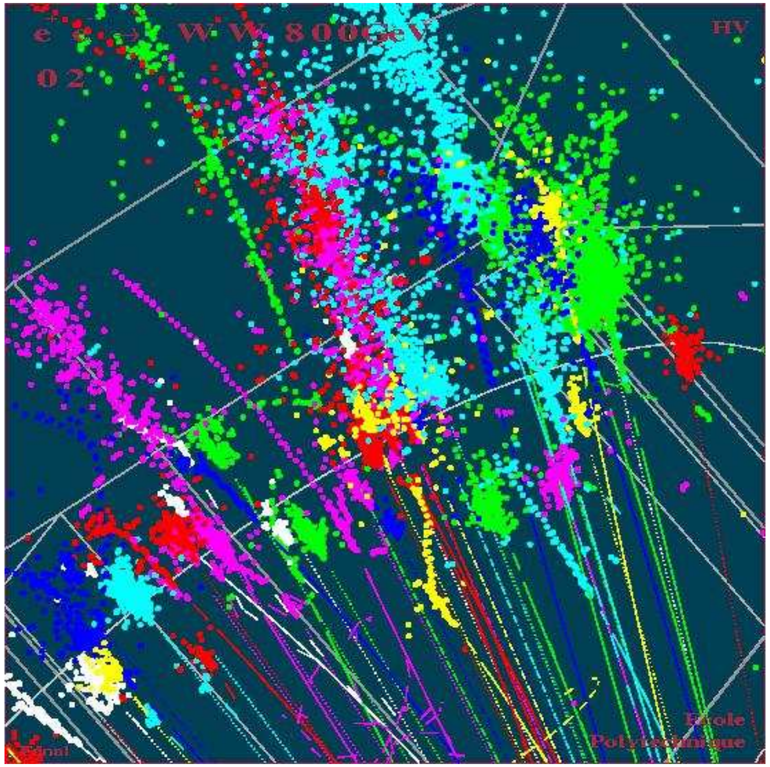

π^+/γ: *Si/W Ecal + RPC/Fe DHcal*

True clusters

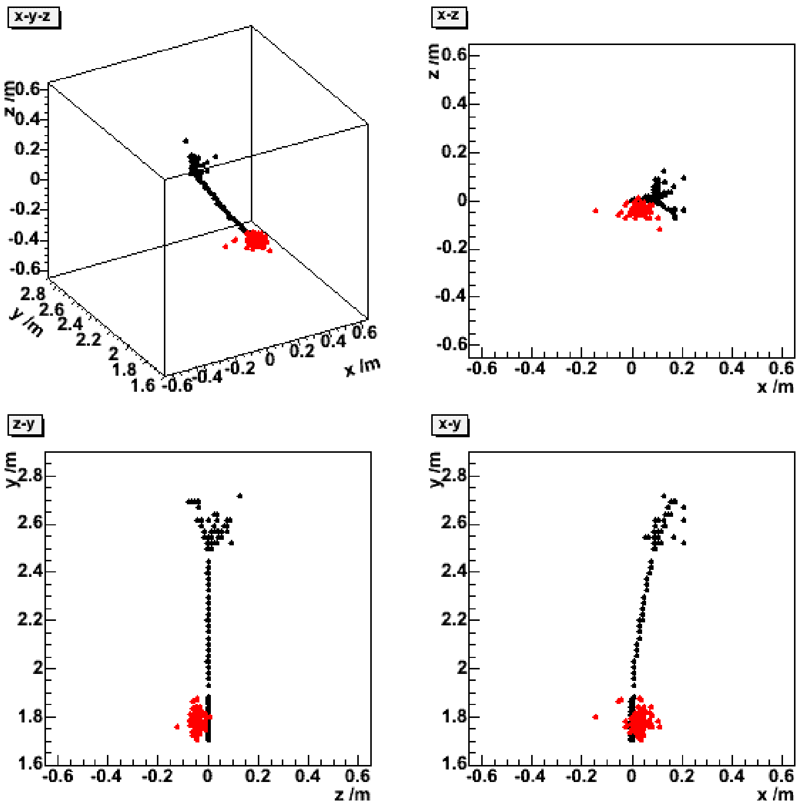

- **Black** cluster = 5 GeV/c π^+.
- **Red** cluster = 5 GeV/c γ.

Reconstructed clusters

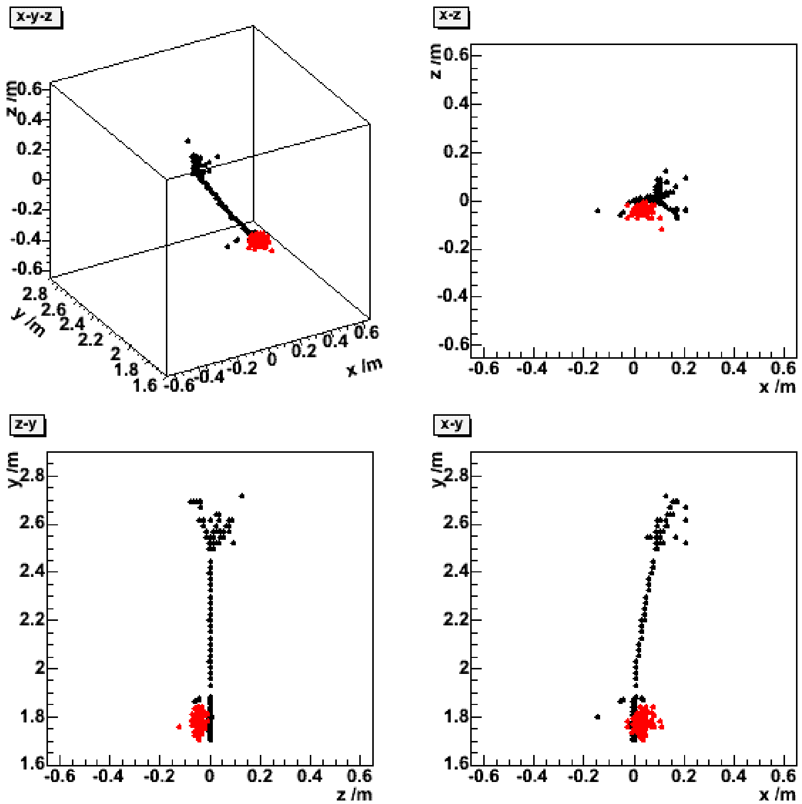

- **Black** cluster matched to charged track.
- **Red** cluster left over as neutral $\Rightarrow \gamma$ energy well reconstructed.

π^+/γ: Si/W Ecal + RPC/Fe DHcal

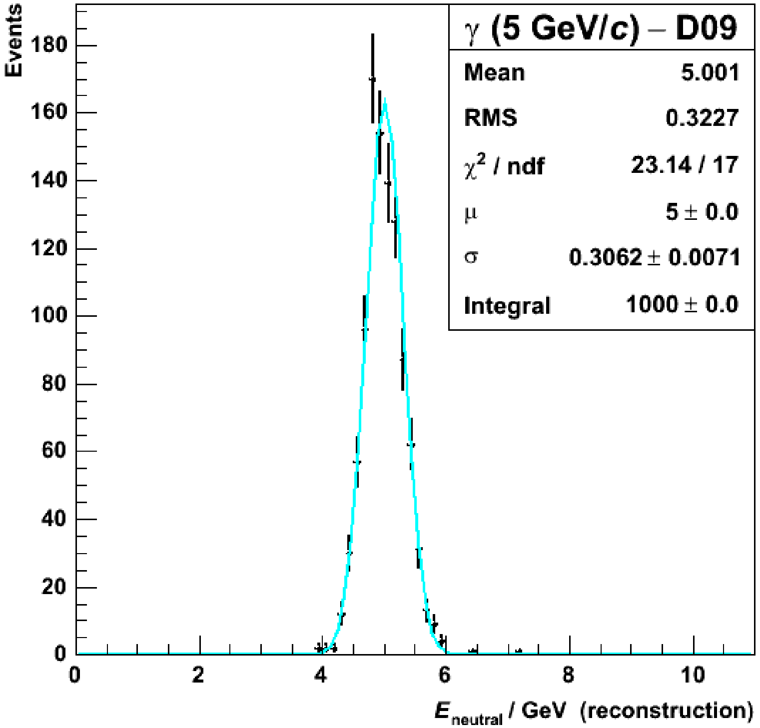

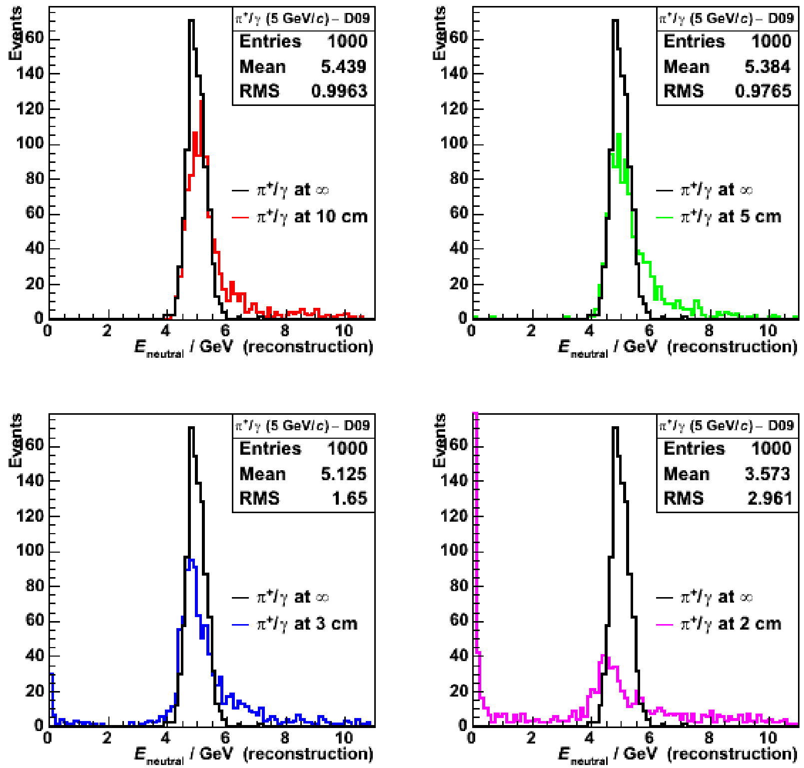

- **1k single γ at 5 GeV/*c*.**
- Fit Gaussian to energy distribution, calibrated according to:
  $E = \alpha[(E_{\text{Ecal; 1-30}} + 3E_{\text{Ecal; 31-40}})/E_{\text{Ecal mip}} + 20N_{\text{Hcal}}]$.
- Fix factors α, 20 by minimising χ^2/dof.
- $\sigma/\sqrt{\mu} \sim 14\% \sqrt{\text{GeV}}$.

- **1k γ with nearby π^+ (10, 5, 3, 2 cm from γ).**
- Peak of photon energy spectrum well reconstructed; improves with separation.
- Tail at higher $E \rightarrow$ inefficiency in π^+ reconstruction.
- Spike at $E = 0$ below 3 cm $\rightarrow$ clusters not distinguished.

π^+/n: Si/W Ecal, RPC/Fe DHcal

True clusters

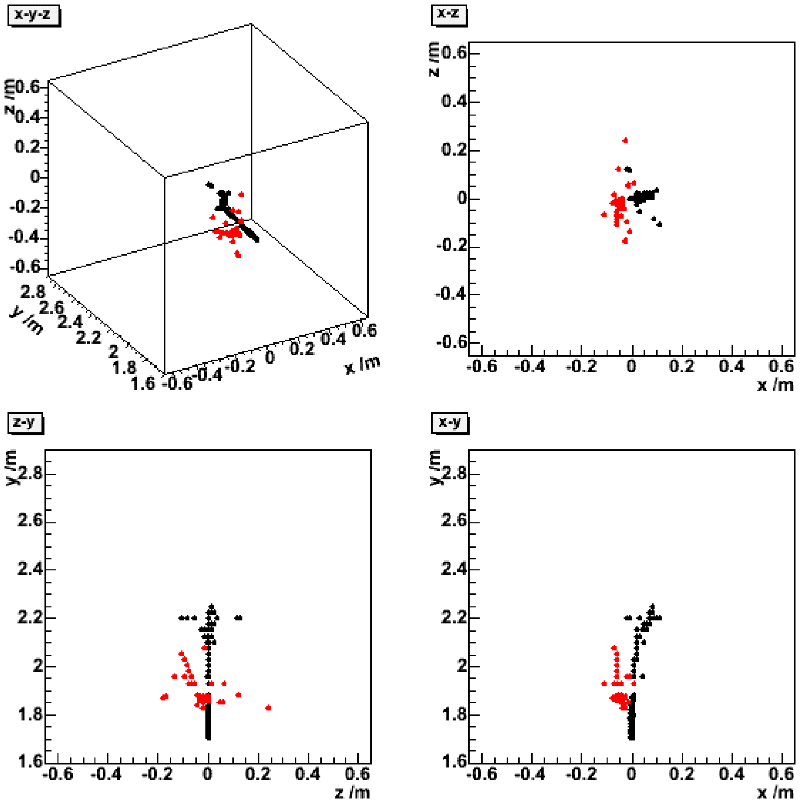

- **Black** cluster = 5 GeV/*c* π^+.
- **Red** cluster = 5 GeV/*c* **n**.

Reconstructed clusters

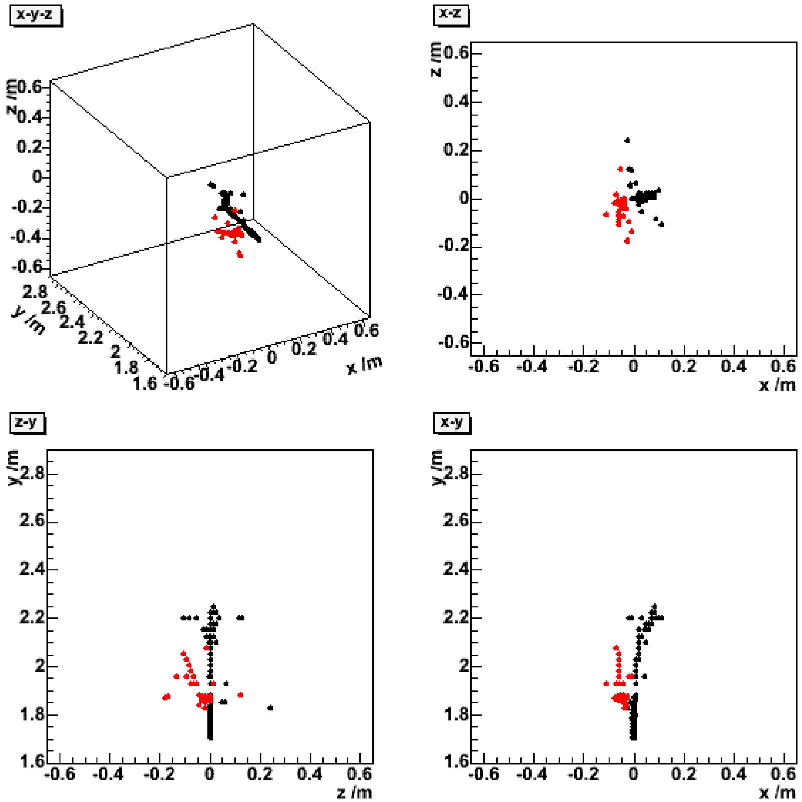

- **Black** cluster matched to charged track.
- **Red** cluster left over as neutral $\Rightarrow$ n energy well reconstructed.

π^+/n: Si/W Ecal, RPC/Fe DHcal

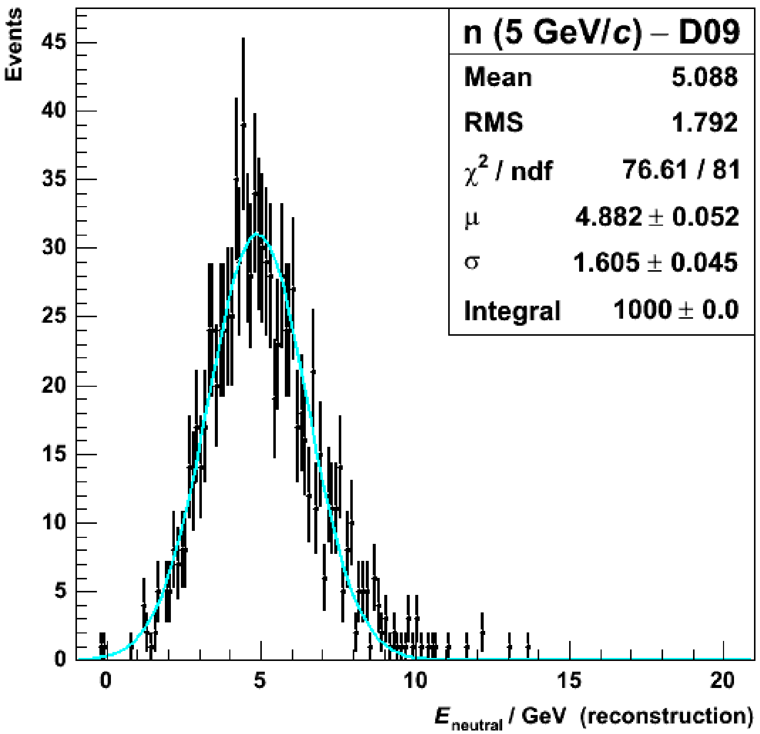

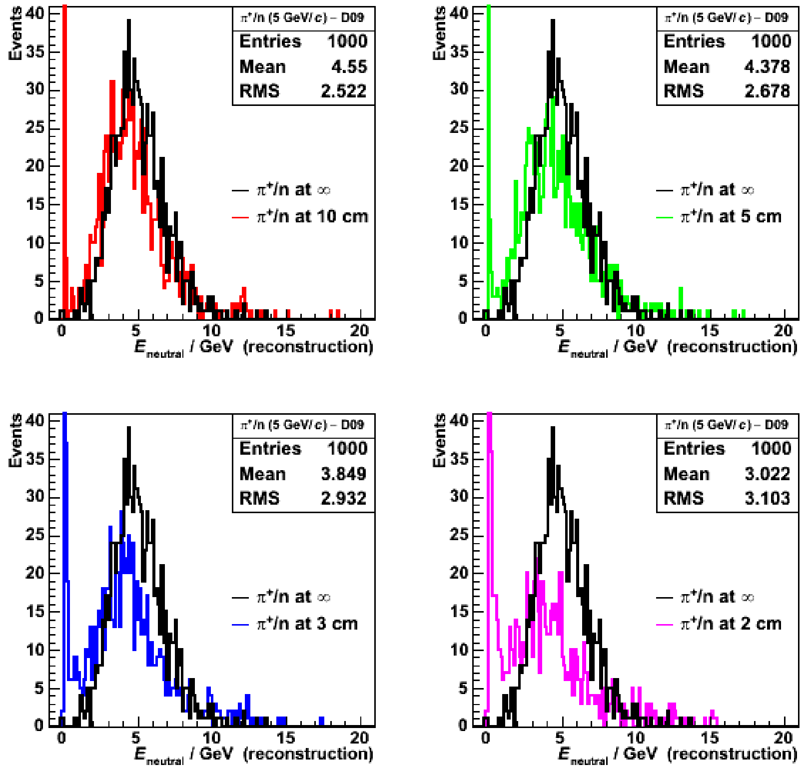

- **1k single n at 5 GeV/*c*.**
- Fit Gaussian to energy distribution, calibrated according to:
  $E = \alpha[(E_{\mathrm{Ecal;\,1\text{-}30}} + 3E_{\mathrm{Ecal;\,31\text{-}40}})/E_{\mathrm{Ecal\ mip}} + 20N_{\mathrm{Hcal}}]$.
- Fix factors α, 20 by minimising χ^2/dof.
- $\sigma/\sqrt{\mu}$ ~ 73% $\sqrt{\mathrm{GeV}}$.

- **1k n with nearby π^+ (10, 5, 3, 2 cm from n).**
- Peak of neutron energy spectrum well reconstructed; improves with separation.
- Spike at $E = 0$ even at 10 cm → clusters not distinguished.

π^+/n: *Si/W Ecal, RPC/Fe Hcal*

True clusters

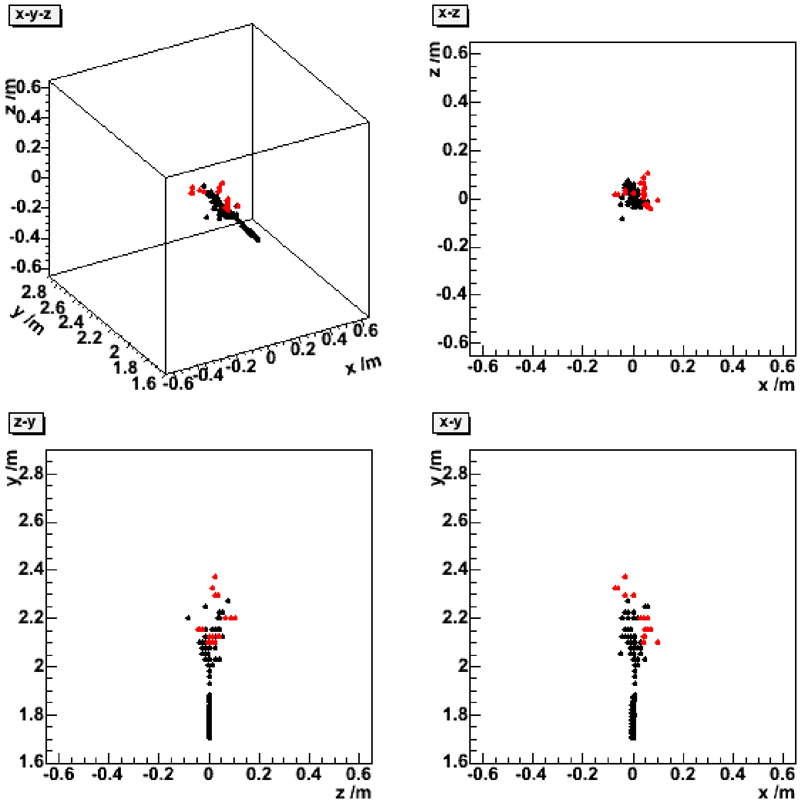

Reconstructed clusters

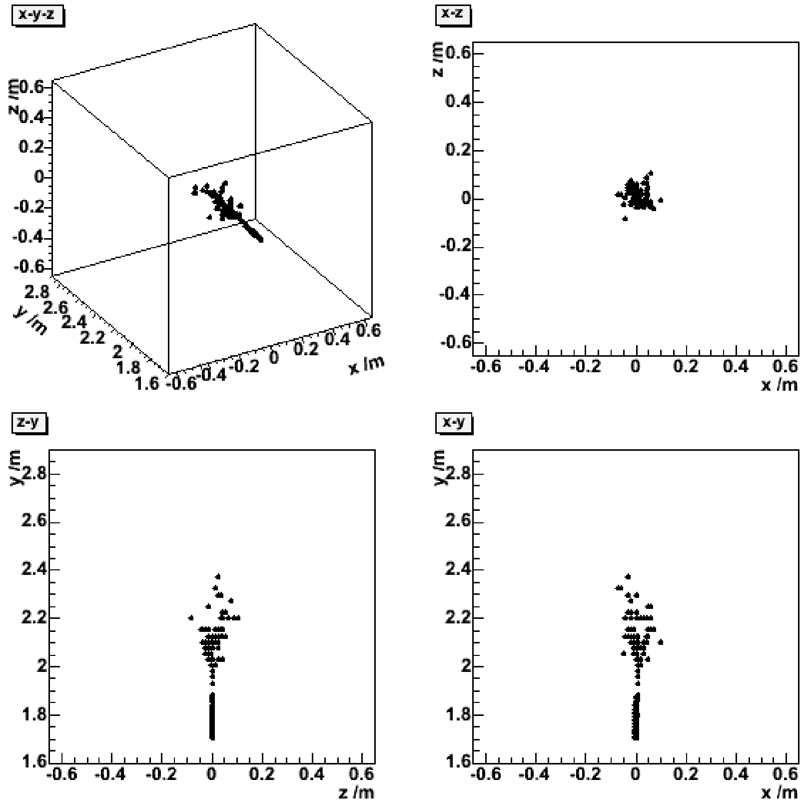

- **Black** cluster = 5 GeV/c π^+.
- **Red** cluster = 5 GeV/c **n**.

- **Black** cluster matched to charged track.
- Nothing left over as neutral $\Rightarrow$ n not reconstructed (*i.e.* $E = 0$).

π^+/γ: Si/W Ecal + scintillator/Fe AHcal

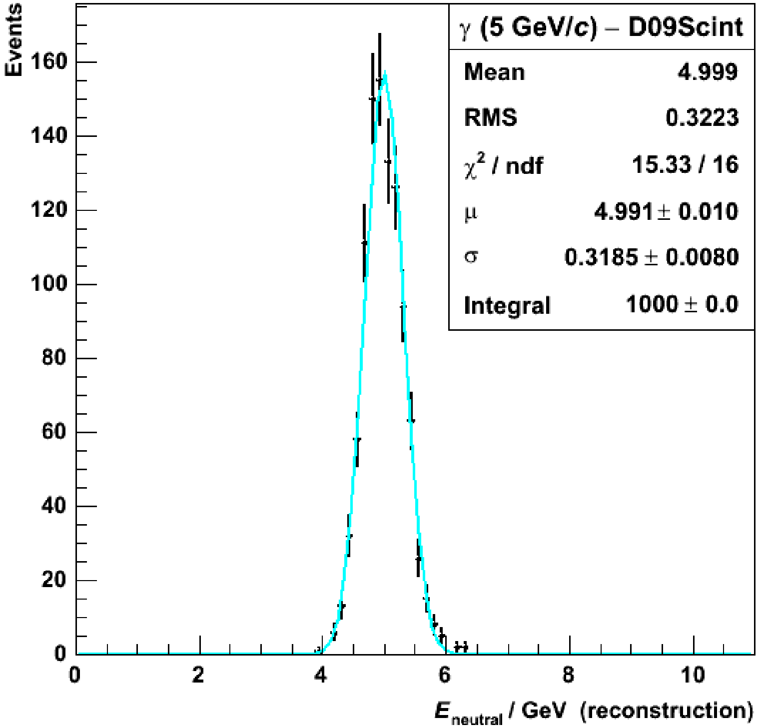

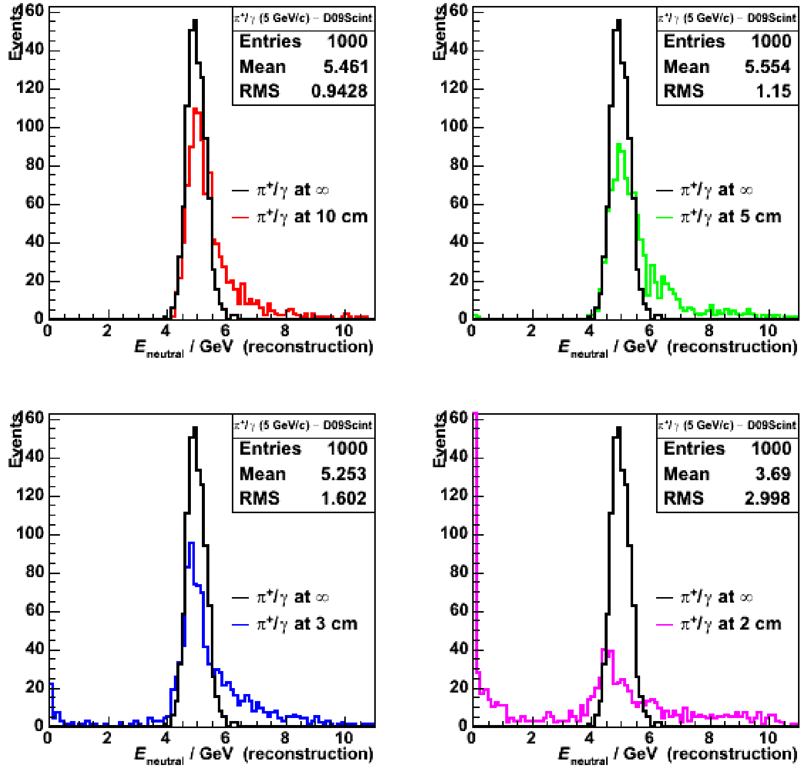

- 1k single γ at 5 GeV/*c*.
- Fit Gaussian to energy distribution, calibrated according to:
  $E = \alpha[(E_{\mathrm{Ecal;\ 1\text{-}30}} + 3E_{\mathrm{Ecal;\ 31\text{-}40}})/E_{\mathrm{Ecal\ mip}} + \mathbf{5}E_{\mathrm{Hcal}}/E_{\mathrm{Hcal\ mip}}]$.
- Fix factors α, **5** by minimising χ^2/dof.
- $\sigma/\sqrt{\mu} \sim 14\% \sqrt{\mathrm{GeV}}$ (as for DHcal).

- **1k γ with nearby π^+ (10, 5, 3, 2 cm from γ).**
- General trends much as for DHcal.

π^+/n: Si/W Ecal + scintillator/Fe AHcal

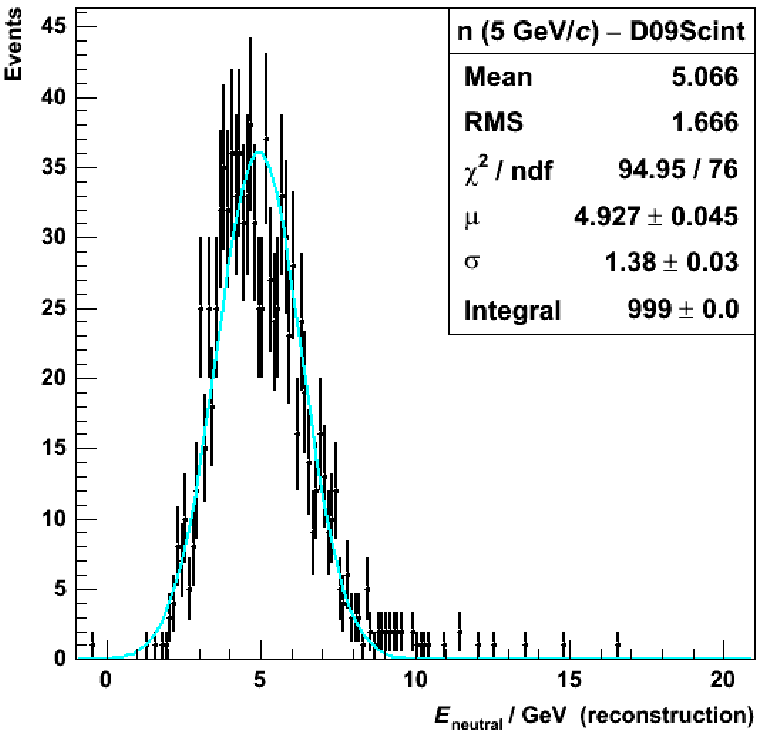

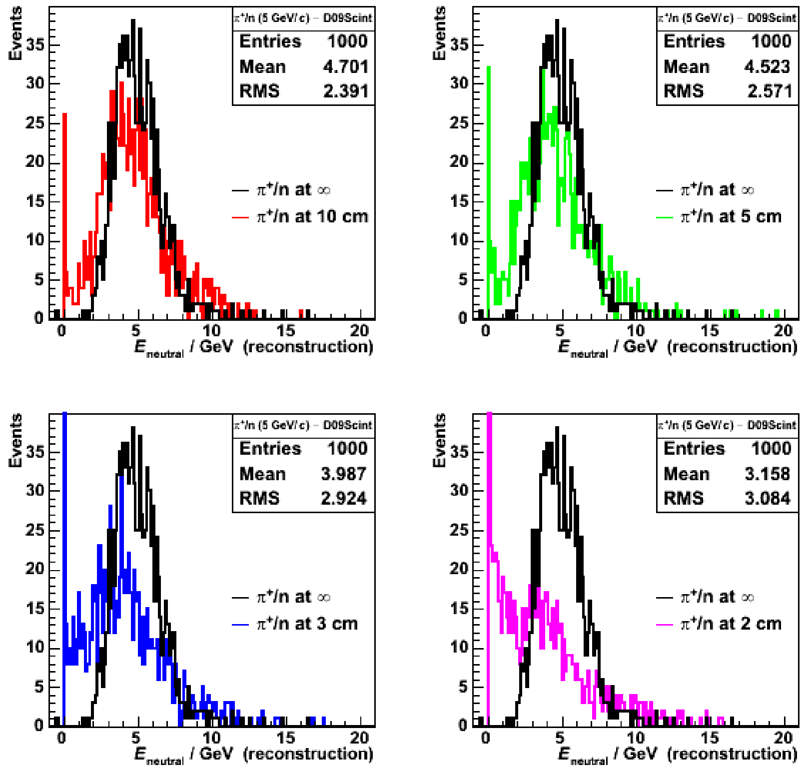

- 1k single **n** at 5 GeV/*c*.
- Fit Gaussian to energy distribution, calibrated according to:
  $E = \alpha[(E_{\text{Ecal; 1-30}} + 3E_{\text{Ecal; 31-40}})/E_{\text{Ecal mip}} + \mathbf{5}E_{\text{Hcal}}/E_{\text{Hcal mip}}]$.
- Fix factors α, **5** by minimising χ^2/dof.
- $\sigma/\sqrt{\mu}$ ~ 62% $\sqrt{\text{GeV}}$ (cf. 73% $\sqrt{\text{GeV}}$ for DHcal).

- **1k n with nearby π^+ (10, 5, 3, 2 cm from n).**
- General trends much as for DHcal.

π^+/neutral cluster separability vs separation

5 GeV/c π^+/γ

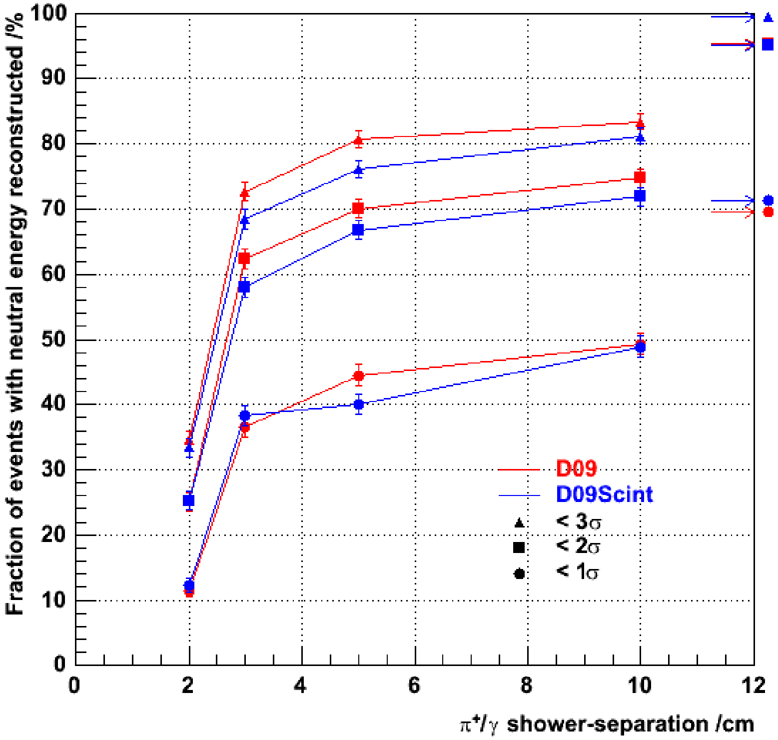

- Fraction of events with photon energy reconstructed within 1,2,3σ generally higher for DHcal ("D09") than for AHcal ("D09Scint").

5 GeV/c π^+/n

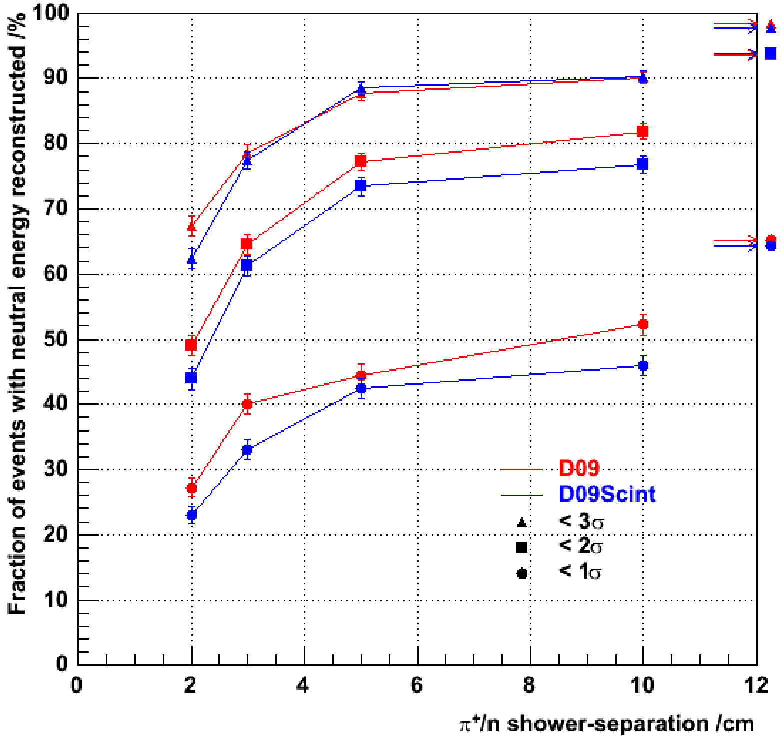

- Similar conclusion for neutrons.
- RPC DHcal favored over scintillator AHcal?
- Needs further investigation…

Conclusions

- ILC: an e^+e^- linear collider operating in the range 0.5–1 TeV.
- Will complement LHC's discovery potential by providing precision measurements.
- Requires unprecedented jet energy resolution.
- Achieved through combination of highly granular calorimetry and particle flow.
- Detector optimization relies on realistic simulation (especially of hadronic showers).
- Needs test beam data for verification.
- CALICE collaboration leading the way.
- For more info, go to **http//:www.hep.phy.cam.ac.uk/calice/**

The OPAL detector

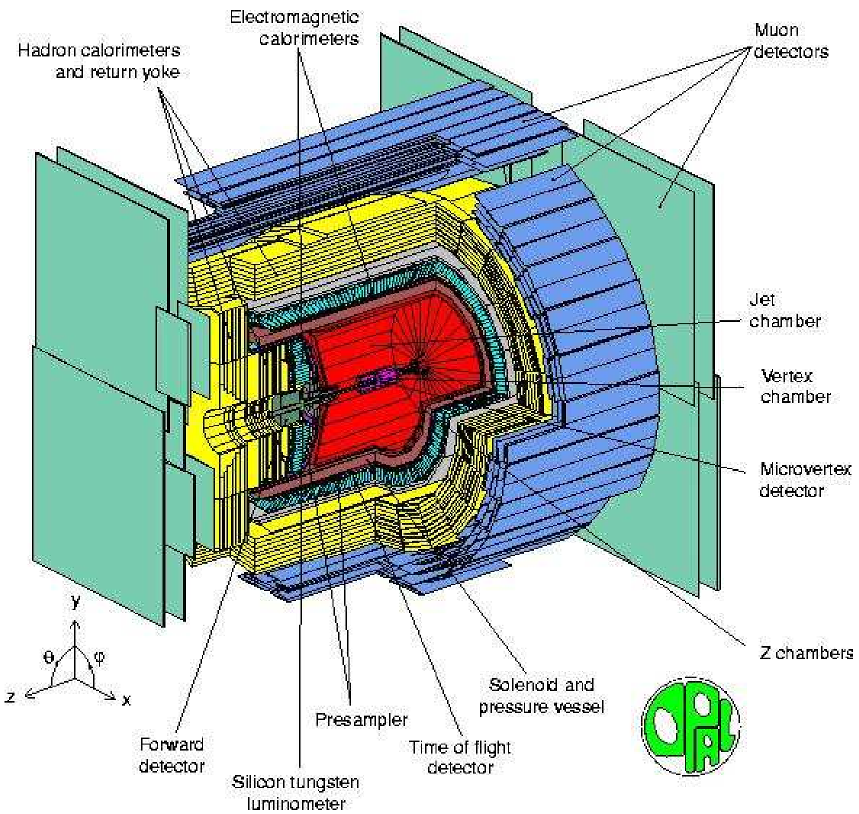

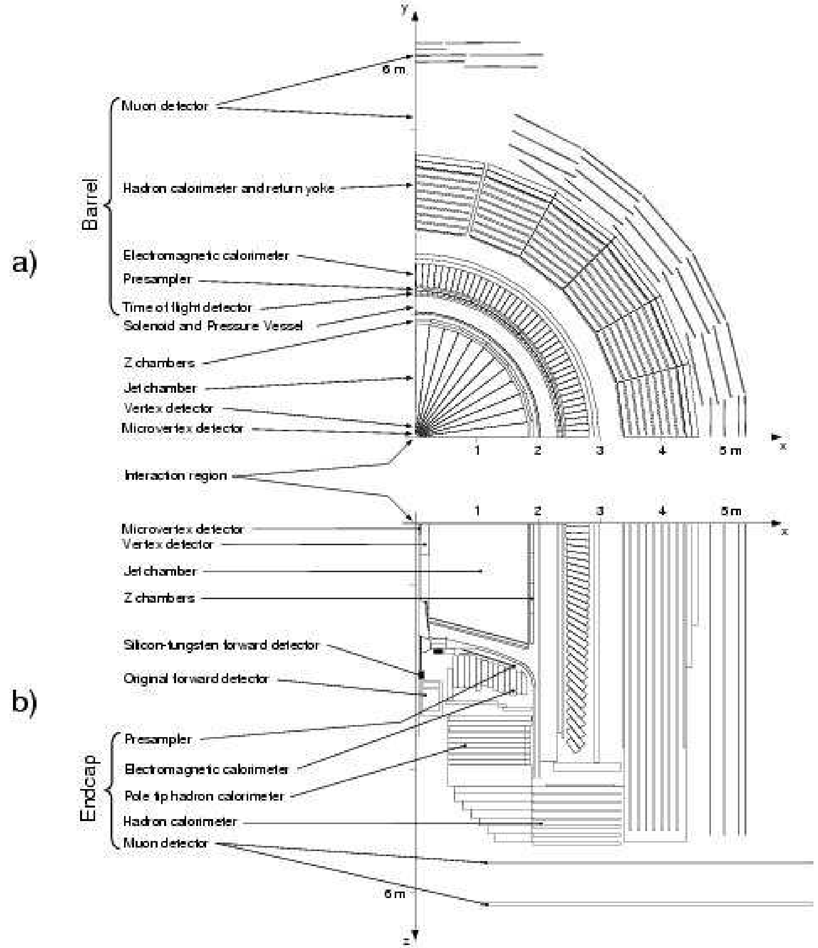

Selection of hadronic events

- High multiplicity cuts to reject leptonic final states:

  $\rightarrow N_{chg} \geq 5$;

  $\rightarrow N_{shw} \geq 7$.

- Visible energy and energy balance cuts to reduce 2-photon and machine backgrounds:

  $$\rightarrow R_{vis} = \frac{\sum E_{shw}}{2E_b} \geq 0.14;$$

  $$\rightarrow |R_{bal}| = \frac{|\sum E_{shw} \cos\theta_{shw}|}{\sum E_{shw}} \leq 0.75.$$

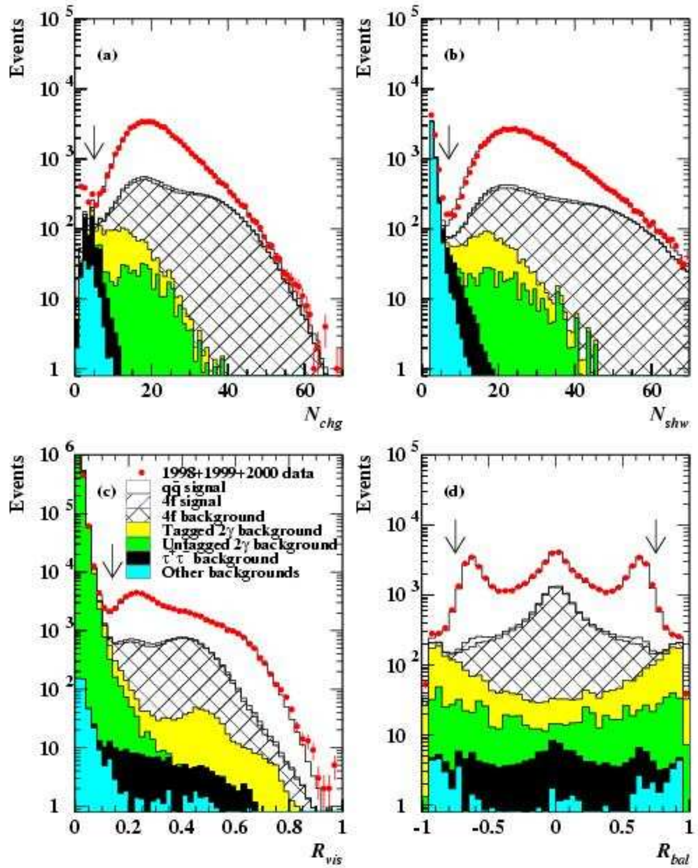

CALICE calorimeter design

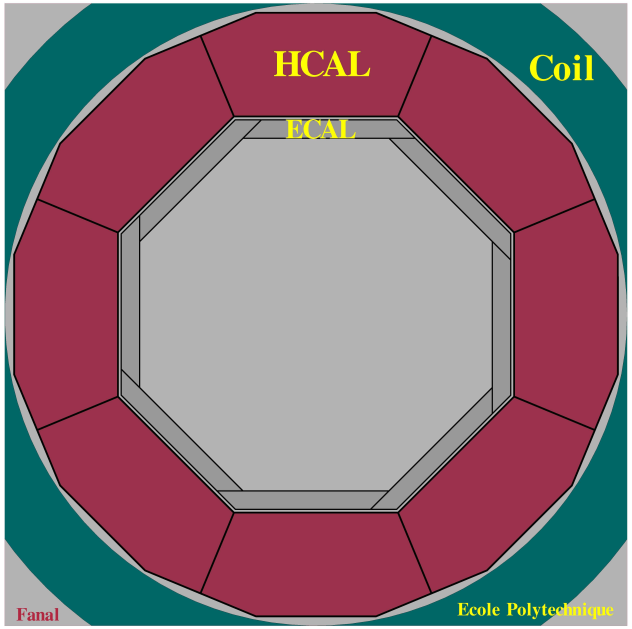

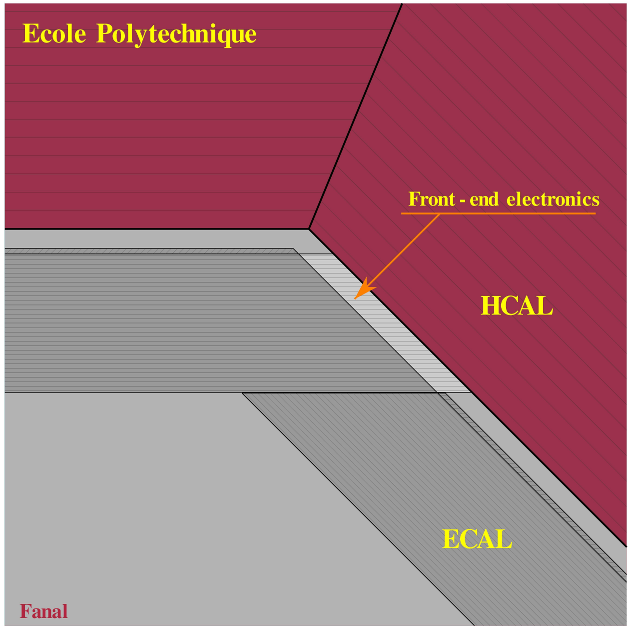

Beam tests

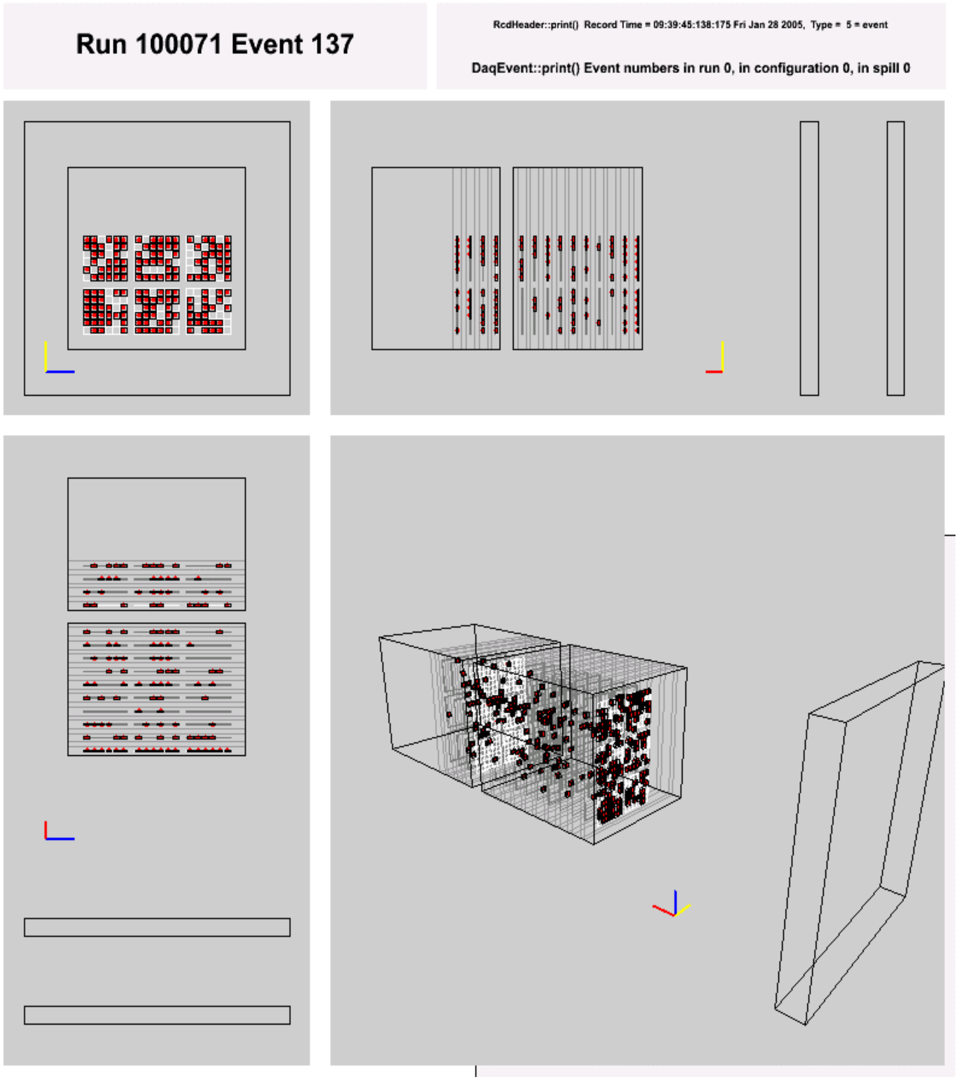

- Cells in red: signal > 20% of mip

Beam tests

- Cells in red: signal > 50% of mip

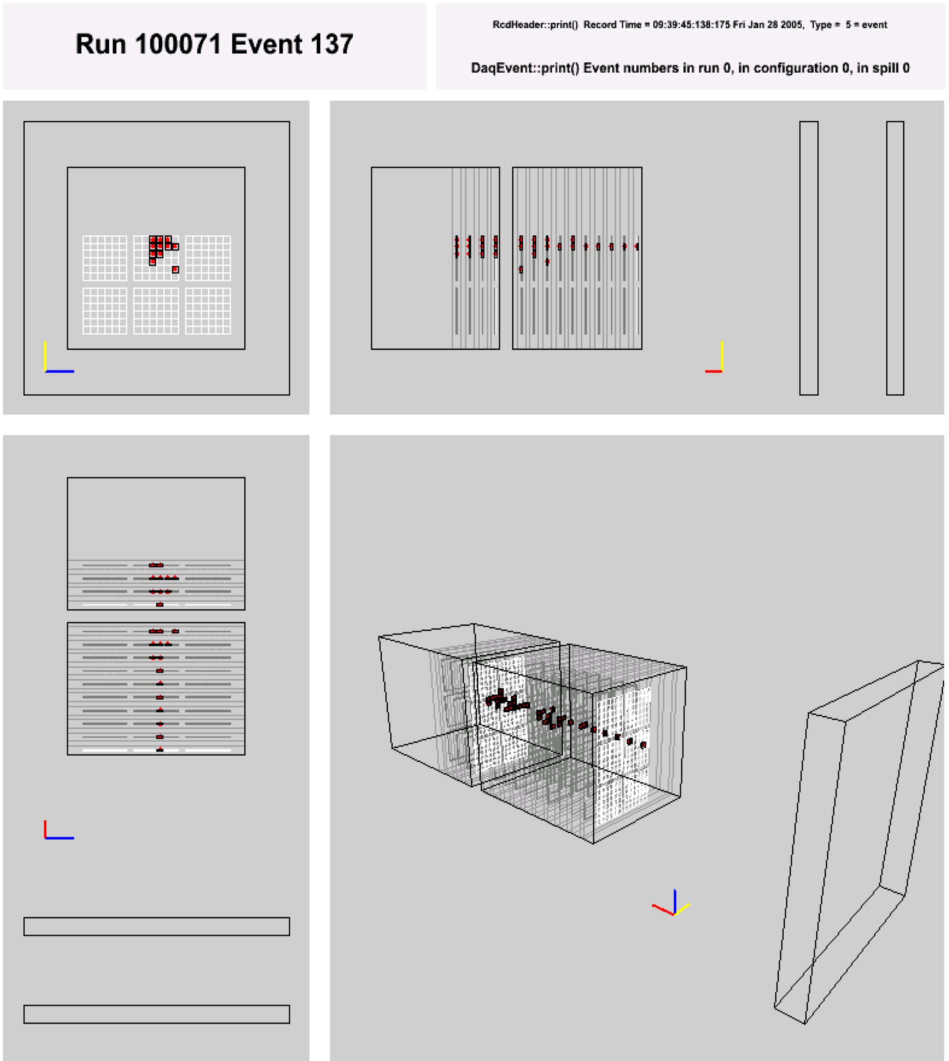

Clustering with MAGIC: stage 1

- Form coarse clusters by ***tracking*** closely-related hits ***layer-by-layer*** through the calorimeter:
  - for a candidate hit in a given layer, l, minimise the distance, d, w.r.t all (already clustered) hits in layer l-1;
  - if $d <$ `distMax` for minimum d, assign candidate hit to same cluster as hit in layer l-1 which yields minimum;
  - if not, repeat with all hits in layer l-2, then, if necessary, layer l-3, *etc.*, right through to layer l-`layersToTrackBack`;
  - after iterating over all hits in layer l, seed new clusters with those still unassigned, grouping those within `proxSeedMax` of hit of highest remaining density into same seed;
  - assign a direction cosine to each layer l hit:
    - if in Ecal, calculate density-weighted centre of each cluster's hits in layer l; assign a direction cosine to each hit along the line joining its cluster's centre in the seed layer (or (0,0,0) if it's a seed) to its cluster's centre in layer l;
    - if in Hcal, assign a direction cosine to each hit along the line from the hit to which each is linked (or (0,0,0) if it's a seed) to the hit itself;
  - iterate outwards through layers.

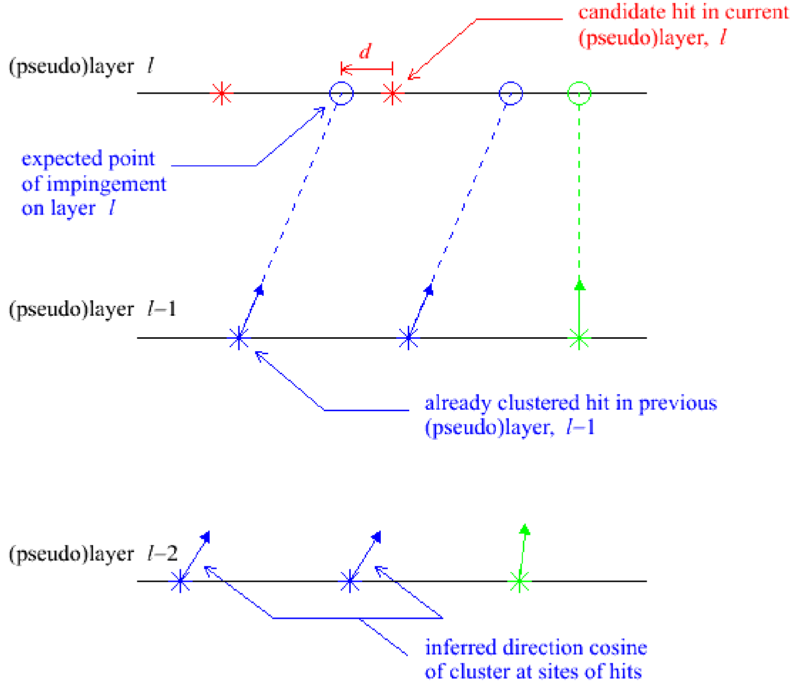

Clustering with MAGIC: stage 2

- Try to merge backward-spiralling track-like cluster-fragments with the forward propagating clusters to which they belong:
  - for each hit in the terminating layer, l, of a candidate cluster fragment, calculate the distance, p, to each hit in nearby clusters in the same layer, and the angle, γ, between their direction cosines;
  - loop over all pairs of hits;
  - if, for any pair, both:
    - p < **proxMergeMax** *and*
    - **cos** γ < **cosGammaMax**

    are satisfied, merge clusters together into one;
  - iterate over clusters.

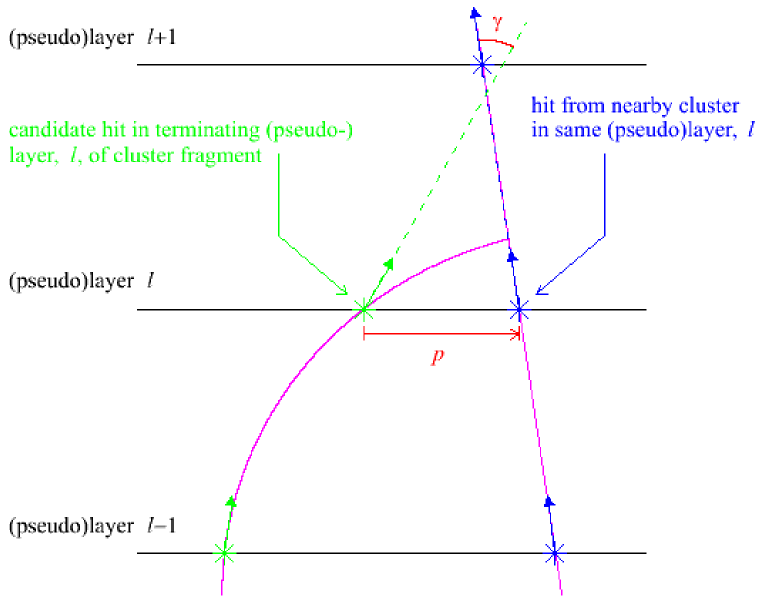

Chris Ainsley
<ainsley@hep.phy.cam.ac.uk>

Clustering with MAGIC: stage 3

- Try to merge low multiplicity cluster "halos" (hit multiplicity < **clusterSizeMin**) which just fail the stage 1 cluster-continuation cuts:
  - for the hit of highest density in the seed layer, ***l***, of a low multiplicity cluster, minimise the angle, β, w.r.t all hits in layer ***l***–1;
  - if **tan** β < **tanBetaMax** for minimum β, merge the clusters containing the repsective hits into one;
  - if not, repeat with all hits in layer ***l***–2, then, if necessary, layer ***l***–3, *etc.*, right through to layer ***l***–**layersToTrackBack**;
  - if still not, repeat above steps with the candidate hit in the seed layer of the low multiplicity cluster of next highest density, *etc.* ;
  - if still not, merge the low multiplicity cluster into the nearest cluster with hits in the same layer as the low multiplicity cluster's seed layer, provided the two clusters contain hits separated by ***s*** < **proxMergeMax**;
  - iterate over clusters.

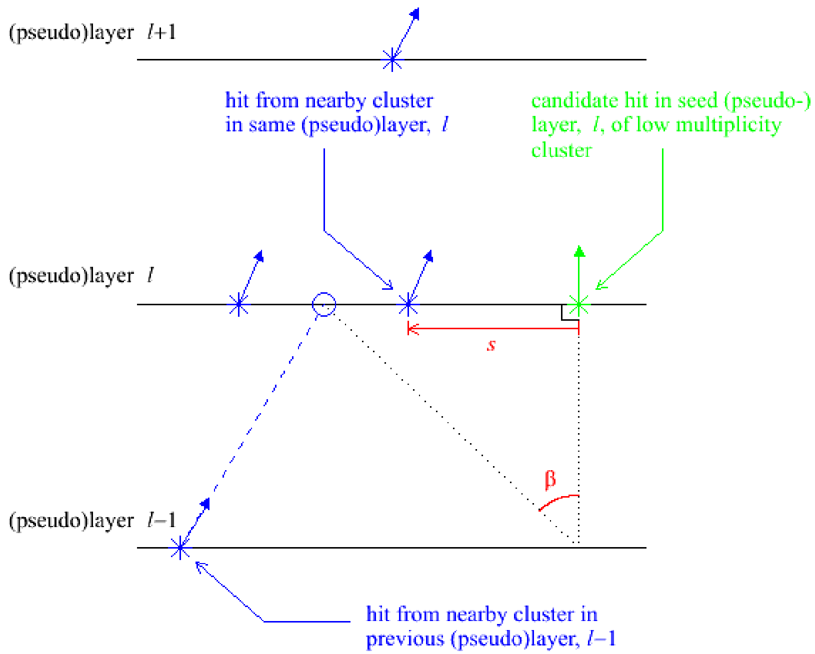

Code organization within LCIO/MARLIN

- Code structured as a series of 5+1 **MARLIN** ***"processors"***, together with a **steering file**: `cluster.steer` (read at ***run-time***).
- Reads hits collections from **LCIO** file, adds **LCIO** clusters collections (essentially pointers back to component hits) and writes everything to new **LCIO** output file.
- Processors to do the reconstruction:
  - `CalorimeterConfigurer`

    → allows user to define geometrical layout of calorimeter;
  - `CalorimeterHitSetter`

    → applies hit-energy threshold and adds pseudolayer and pseudostave indices to hits collection (encoded in CellID1 akin to encoding of layer and stave indices in CellID0) as well as hit weights (= local hit density);
  - `CalorimeterStage1Clusterer`

    → performs coarse cluster reconstruction;
  - `CalorimeterStage2Clusterer`

    → recovers backward-spiralling track-like cluster fragments;
  - `CalorimeterStage3Clusterer`

    → recovers low multiplicity cluster fragments.
- Additional processor to access MC truth (if simulation):
  - `CalorimeterTrueClusterer`

    → constructs true clusters, where a true cluster is considered to comprise all hits attributable to either:

    (i) the same generator primary or any of its non-backscattered progeny, or

    (ii) the same backscattered daughter or any of its non-backscattered progeny.

User-controlled steering with MARLIN

- Detector parameters and clustering cuts set in **cluster.steer** (e.g. Mokka D09 model):

```
ProcessorType CalorimeterConfigurer
     detectorType             full        # "full" => barrel+endcaps; "prototype" => layers perp'r to +z
     iPx                      0.          # x-coordinate of interaction point (in mm)
     iPy                      0.          # y-coordinate of interaction point (in mm)
     iPz                      0.          # z-coordinate of interaction point (in mm)
     ecalLayers               40          # number of Ecal layers
     hcalLayers               40          # number of Hcal layers
     barrelSymmetry           8           # degree of rotational symmetry of barrel
     phi_1                    90.0        # phi offset of barrel stave 1 w.r.t. x-axis (in deg)
ProcessorType CalorimeterHitSetter
     ecalMip                  0.000150    # Ecal MIP energy (in GeV)
     hcalMip                  0.0000004   # Hcal MIP energy (in GeV)
     ecalMipThreshold         0.3333333   # Ecal hit-energy threshold (in MIP units)
     hcalMipThreshold         0.3333333   # Hcal hit-energy threshold (in MIP units)
ProcessorType CalorimeterStage1Clusterer
     layersToTrackBack_ecal   3           # number of layers to track back in Ecal
     layersToTrackBack_hcal   3           # number of layers to track back in Hcal
     distMax_ecal             20.0        # distance cut in Ecal (in mm)
     distMax_hcal             30.0        # distance cut in Hcal (in mm)
     proxSeedMax_ecal         14.0        # maximum cluster-seed radius in Ecal (in mm)
     proxSeedMax_hcal         50.0        # maximum cluster-seed radius in Hcal (in mm)
ProcessorType CalorimeterStage2Clusterer
     proxMergeMax_ecal        20.0        # Ecal proximity cut for cluster merging (in mm)
     proxMergeMax_hcal        30.0        # Hcal proximity cut for cluster merging (in mm)
     cosGammaMax              0.5         # angular cut for cluster merging
ProcessorType CalorimeterStage3Clusterer
     clusterSizeMin           10          # minimum cluster size to avert potential merging
     layersToTrackBack_ecal   39          # number of layers to track back in Ecal for merging
     layersToTrackBack_hcal   79          # number of layers to track back in Hcal for merging
     tanBetaMax               6.0         # angular cut for cluster merging
     proxSeedMax_ecal         400.0       # Ecal proximity cut for cluster merging (in mm)
     proxSeedMax_hcal         400.0       # Hcal proximity cut for cluster merging (in mm)
```

Getting started with MAGIC

- Install **LCIO** (≥ v01-05) and **MARLIN** (≥ v00-07).
- Download *MAGIC* tar-ball from
  `http://www.hep.phy.cam.ac.uk/~ainsley/MAGIC/MAGIC-v01-02.tar.gz`
- **Two directories** and a **README** file (read this first!).
- The `clustering` **directory** contains the cluster-reconstruction (and cluster-truth) code (i.e. all processors and steering file mentioned earlier).
- Takes **.slcio input** files containing `CalorimeterHits` (data) or `SimCalorimeterHits` (MC):
  - must be generated with hit-positions stored, *i.e.* `RCHBIT_LONG=1` (data) or `CHBIT_LONG=1` (MC);
  - collection names must contain the string "`ecal`" or "`hcal`" (in upper or lower case, or in some combination of these) to identify the type of hit (for energy-threshold application).
- Produces **.slcio output** file with cluster-related collections added:
  - `CalorimeterHits` ⇒ hits above energy threshold;
  - `CalorimeterHitRelationsToSimCalorimeterHits` (**MC only**) ⇒ pointers to original simulated hits;
  - `CalorimeterStage1Clusters` ⇒ clusters after stage 1 of algorithm;
  - `CalorimeterStage2Clusters` ⇒ clusters after stage 2 of algorithm;
  - `CalorimeterStage3Clusters` ⇒ clusters after stage 3 of algorithm;
  - `CalorimeterTrueClusters` (**MC only**) ⇒ true clusters;
  - `CalorimeterTrueClusterRelationsToMCParticles` (**MC only**) ⇒ pointers to original MC particles.
- The `examples` **directory** contains example analysis code which performs simple manipulations with the clusters (e.g. processors which add calibrated energies to clusters, produce the plots shown earlier, calculate the reconstruction quality… and an accompanying steering file).

Generalising the calorimeter (1)

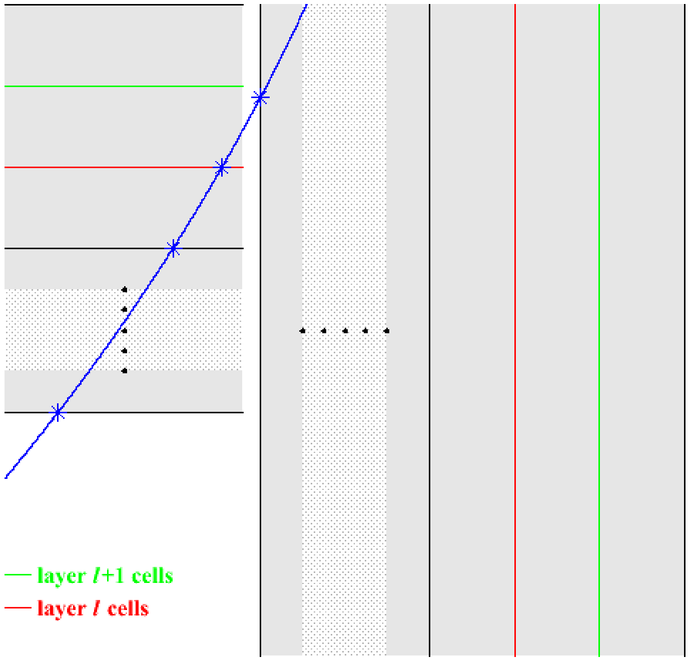

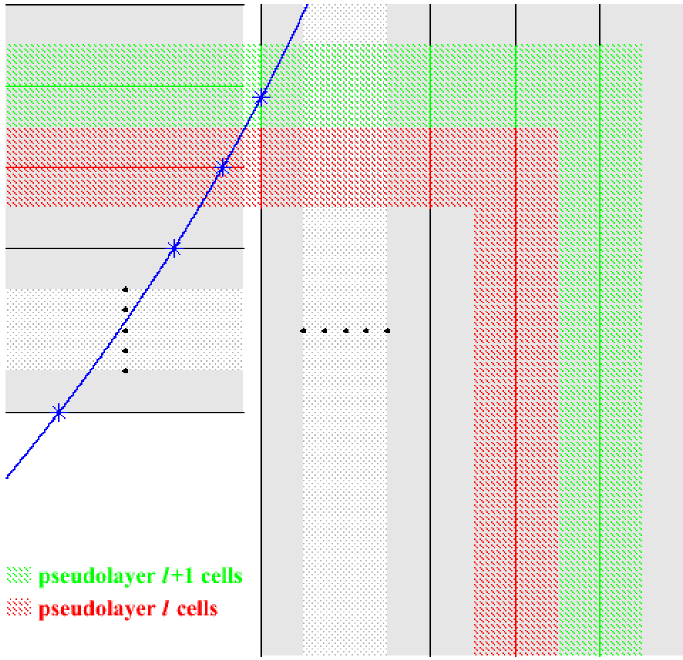

- Layer index changes discontinuously at barrel/endcap boundary.
- On crossing, jumps from l to 1 (first Ecal layer).

- Define a "***pseudolayer***" index based on projected intersections of physical layers.
- Index varies smoothly across boundary.
- Pseudolayer index = layer index, *except* in overlap region.

Generalising the calorimeter (2)

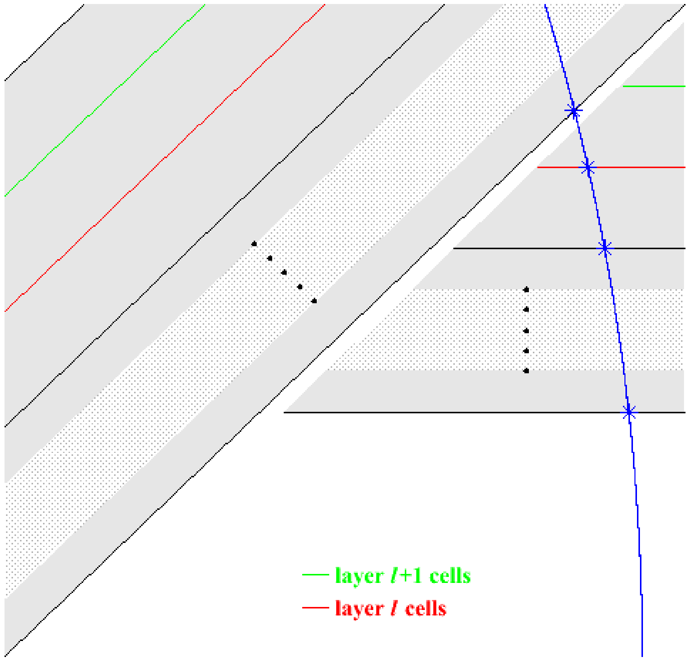

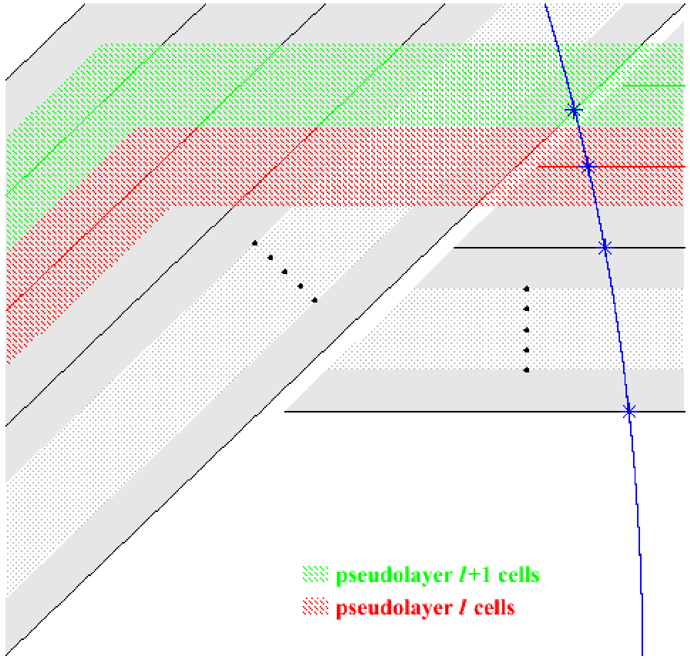

- Layer index changes discontinuously at boundary between overlapping barrel staves.
- On crossing, jumps from ***l*** to 1 (first Ecal layer.

- Again, define "***pseudolayer***" index from projected intersections of physical layers.
- Again, index varies smoothly across boundary.
- Again, pseudolayer index = layer index, *except* in overlap region.

Generalising the calorimeter (3)

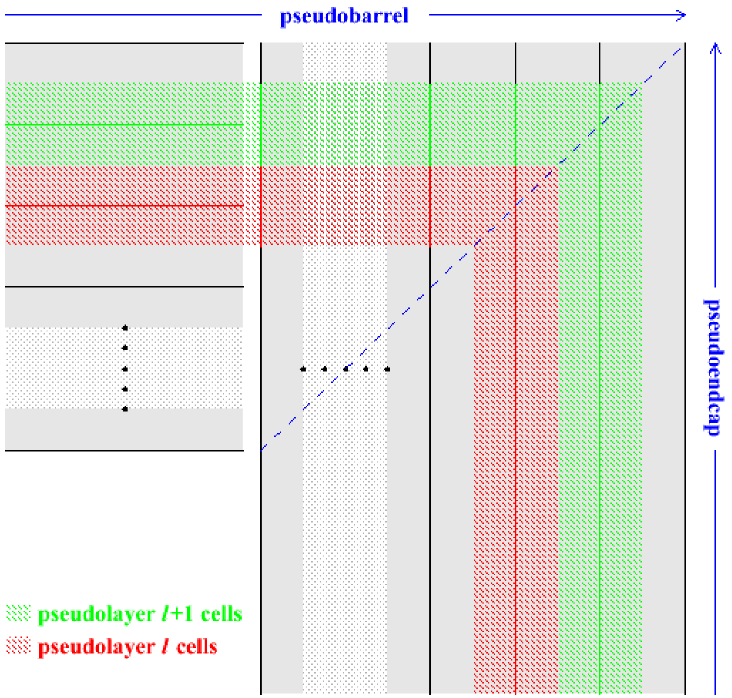

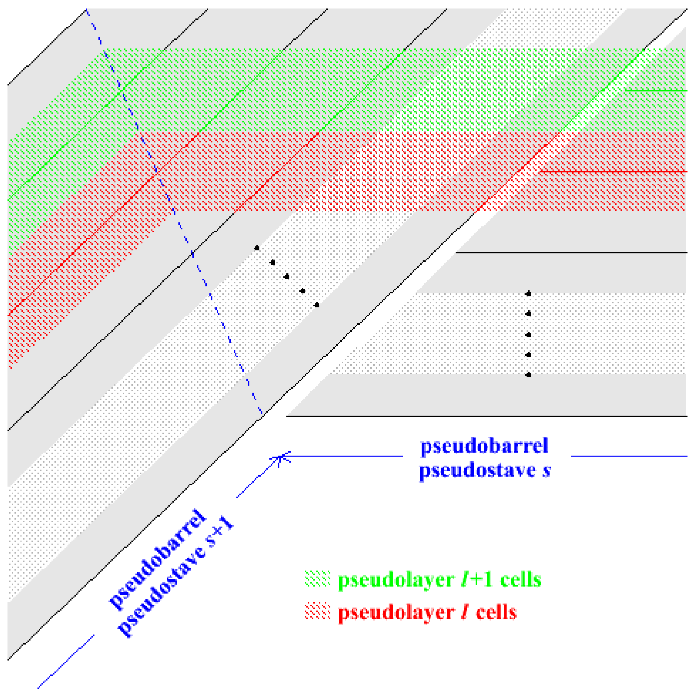

- Define a ***"pseudostave"*** as a plane of parallel pseudolayers.
- ***"Pseudobarrel"*** pseudostaves meet boundaries with left- and right-hand ***"pseudoendcap"*** pseudostaves along 45° lines (if layer-spacings equal in barrel and endcaps).

- ***"Pseudobarrel"*** pseudostaves meet boundaries with other ***"pseudobarrel"*** pseudostaves along 360°/2***n*** lines (for an ***n***-fold rotationally symmetric barrel).
- Calorimeter divides naturally into ***n*+2** pseudostaves.

Generalising the calorimeter (4)

- Code recasts any layered calorimeter composed of a rotationally symmetric barrel closed by two endcaps into this standard, generalised form comprising layered shells of rotationally-symmetric ***n***-polygonal prisms, coaxial with *z*-axis.
- Layers and staves from which calorimeter is built translated into pseudolayers and pseudostaves with which algorithm works.
- Only required inputs as far as algorithm is concerned are:
  - **`barrelSymmetry`** = rotational symmetry of barrel (***n***);
  - **`phi_1`** = orientation of pseudobarrel pseudostave 1 w.r.t. *x*-axis;
  - **`distanceToBarrelLayers[ecalLayers+hcalLayers+2]`**
    = layer positions in barrel layers ("**+2**" to constrain inside edge of first pseudolayer and outside edge of last pseudolayer); and
  - **`distanceToEndcapLayers[ecalLayers+hcalLayers+2]`**
    = layer positions in endcap layers;

$\rightarrow$ as geometry-independent as it's likely to get!

Example event: Z → u,d,s jets at 91 GeV

Reconstructed clusters | **True clusters**

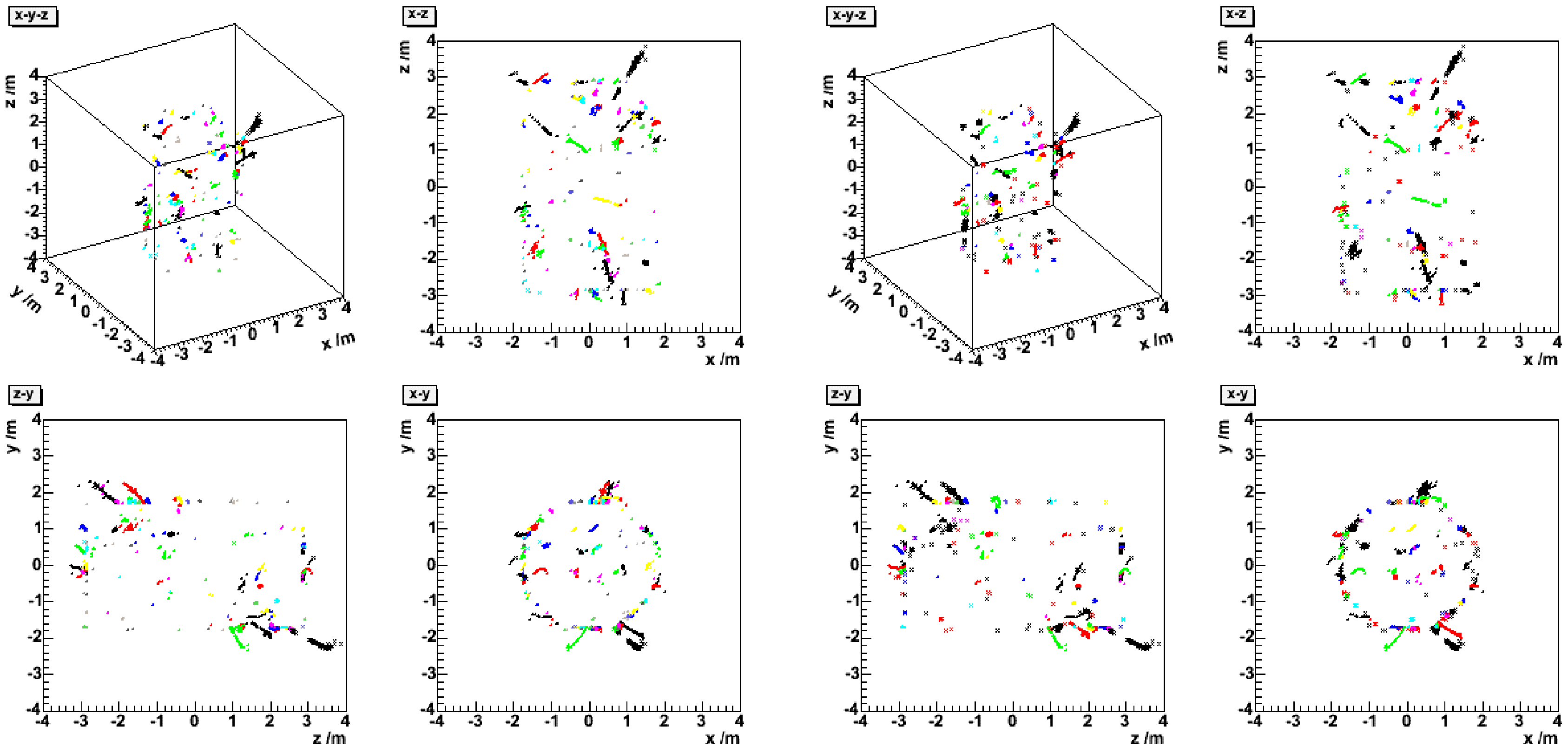

- Reconstruction works successfully not only for ***intra***-stave, but also for ***inter***-stave clusters (*e.g.* ***black*** truth cluster spanning barrel staves 5+6 and the RH endcap correctly reconstructed).